Complex manifolds for the Euler equations: a hierarchy of ODEs and the case of vanishing angle in two dimensions

Andrew D. Gilbert [a] and Walter Pauls [b]

[a] *Mathematics Research Institute, College of Engineering, Mathematics and Physical Sciences, University of Exeter, EX4 4QF, U.K.*

[b] *Max Planck Institute for Dynamics and Self-Organization, Göttingen, Germany.*

Abstract

This paper considers the two-dimensional Euler equations for complex spatial variables and two complex modes in the initial condition. A hierarchy of third order ODEs is used to study the location and structure of the complex singular manifold for short times. The system has two key parameters, the ratio η of the wave numbers of the two modes, and the angle ϕ between the two wave vectors. Using this hierarchy for the case $\phi = \pi/2$ the results of earlier authors (Pauls *et al. Physica D* **219**, 40–59) are reproduced numerically.

To make analytical progress, the paper considers the limit $\phi \to 0$ in which the wave vectors become parallel, rescaling time also. By considering the limiting behaviour of the ODE hierarchy, an asymptotic framework is set up that describes the geometry of the singular manifold and local behaviour of vorticity in this limiting case $\phi = 0$ of parallel modes.

In addition, the hierarchy of ODEs can be solved analytically, order by order, in the parallel case using computer algebra. This is used to confirm the asymptotic theory and to give evidence for a scaling exponent $\beta = 1$ for the blow-up of vorticity on the singular manifold, $\omega = O(s^{-\beta})$ in this case of vanishing angle ϕ.

Key words: Euler equation, complex manifold, singularity, scaling exponent

1 Introduction

The question of whether finite-time singularities can form in the Euler equation in three dimensions remains a major challenge to mathematics, with a

wide range of approaches and tools being employed. Numerical simulations of the Euler equations have yet to obtain firm evidence of singularity formation at some time t_* from smooth initial conditions, or of flows staying smooth forever, and it is clear that unambiguous numerical identification of this can only be achieved in concert with analytical models and estimates (Kerr, 2005; Hou & Li, 2006; Grafke *et al.*, 2007; Gibbon, Bustamante & Kerr, 2008). Blow-up of vorticity through vortex stretching has been seen in idealised models, for example replacing vorticity fields by tubes of simplified cross-section and the use of truncated dynamics (Moffatt, 2000; Pelz, 2001; Childress, 2008). However the dynamics of vorticity is complicated, and processes such as flattening of vortex tubes can yield structures that are not easily described by idealised or asymptotic models. At the same time flattening can reduce much of the stretching seen in the idealised models, a process termed depletion, slowing the reduction of scales and delaying the onset of a singularity, possibly forever. Another approach is to understand regularity in a functional analytical setting (Deng, Hou & Yu, 2005; Chae, 2006; Constantin, 2007; He, 2007). This has yielded many useful necessary conditions for loss of regularity, most famously the Beale, Kato & Majda (1984) condition, that can then be fed into numerical simulations and models (Bustamante & Kerr, 2008; Hou & Li, 2008). Our purpose is not to review all these approaches, and beyond the few representative references given above we direct the reader to Frisch, Matsumoto & Bec (2003) and Gibbon (2008) for comprehensive bibliographies.

One attractive means of attack is not to wait for singularities to emerge at some time in the real, phase space of the fluid, but instead to characterise and track singularities in complex space. The idea is to start with an initial flow $\boldsymbol{u}(\boldsymbol{x}, 0)$ at $t = 0$, depending on the spatial coordinates $\boldsymbol{x} = (x_1, x_2, x_3)$ and to extend it by analytic continuation to depend on corresponding complex coordinates $\boldsymbol{z} = (z_1, z_2, z_3)$. For example, we can choose an initial condition that is entire in these complex coordinates, such as the Taylor–Green vortex or Kida–Pelz flow (Taylor & Green, 1937; Kida, 1985; Pelz & Gulak, 1997). As time t (which is always taken to be real) increases, generally the solution will develop singularities in complex space and we can define the width $\delta_{\mathrm{an}}(t)$ of the analyticity strip, the distance from real values of the coordinates to the nearest singularity with respect to the complexified coordinates. Initially $\delta_{\mathrm{an}}(0) = \infty$ and if at a finite time t_* in the future, $\delta_{\mathrm{an}}(t_*) = 0$, we have a singularity in real space at this time.

The main mathematical results in this area go back to Benachour (1976, 1979) and Bardos & Benachour (1977), and for our purposes the key point is that the width $\delta_{\mathrm{an}}(t)$ of the analyticity strip is upper semi-continuous. Thus any singularity that appears at some finite time t_* in real space must have had a presence in the complex space at earlier times: it cannot appear 'out of the blue', to quote Frisch, Matsumoto & Bec (2003), who give more detailed discussion. Starting with entire data, the complex singularities must emerge from

infinity and generally at time $t > 0$ they will be present, with $\delta_{\rm an}(t)$ diverging with t as $t \to 0^+$, for example as $\log t^{-1}$ in the examples of the present paper, and in even simpler situations such as passive scalar advection in Lagrangian coordinates (Pauls & Matsumoto, 2005). They then move inwards: in the case of two-dimensional Euler flow, it is well known that $\delta_{\rm an}(t)$ remains positive and no singularity ever reaches the real axis. In three dimensions this approach provides a tool to study the onset of possible singularities in large-scale numerical simulations, by extracting $\delta_{\rm an}(t)$ from information about the exponential fall-off of the energy spectrum of the flow. In Sulem, Sulem & Frisch (1983) this approach was advocated, and applied to several equations including the two-dimensional Euler equation. It was first used for the three-dimensional Taylor–Green vortex in Brachet *et al.* (1983) and more recently in Brachet *et al.* (1992) and Cichowlas & Brachet (2005): the results appear consistent with an exponential decay of $\delta_{\rm an}(t)$ in time. We note that complex singularities are also discussed in the context of axisymmetric, swirling flows by Caflisch (1993) and in Navier–Stokes flows by Li & Sinai (2008).

To gain more of an analytical handle on such complex singularities, and to go beyond large-scale numerical simulations, a series of papers investigates the case of the two-dimensional Euler equations (Frisch, Matsumoto & Bec, 2003; Matsumoto, Bec & Frisch, 2005, 2008; Pauls & Matsumoto, 2005; Pauls *et al.*, 2006; Pauls, 2009). Of course in this case no real-space singularity can occur, and $\delta_{\rm an}(t) > 0$ for all time t. However this problem is much simplified compared with the three-dimensional case, and so this is an important test bed as part of a programme to eventually move into three dimensions. The aim is to characterise singularities, their motion, interaction and any universality properties. In addition, information is obtained about the process of depletion, how the vorticity field can evolve to reduce the effect of nonlinearity so delaying the onset of small scales in two dimensions, or possible singularities in three.

Of this group of studies of complex singularities in two dimensions, the present paper builds on the papers Pauls *et al.* (2006), henceforth referred to as PMFB, and Pauls (2009), henceforth referred to as WP. PMFB studies the structure of complex singularities of the Euler equations, beginning with just two complex Fourier modes in two-dimensional, periodic space (x_1, x_2). In this case although the initial flow is entire as function of the complex coordinates $\boldsymbol{z} = (z_1, z_2)$ at $t = 0$, for $t > 0$ singularities emerge at a distance $\delta_{\rm an} = O(\log t^{-1})$ away. By fixing the real parts $\boldsymbol{x}$ of the coordinates $\boldsymbol{z} = \boldsymbol{x} + i\boldsymbol{y}$ appropriately, PMFB map the structure of the flow as a singular manifold in the plane of the imaginary coordinates $\boldsymbol{y}$ governed by a 'pseudo-hydrodynamic' equation involving vorticity transport and Rayleigh friction. Using very high precision arithmetic the amplitudes of Fourier modes can be calculated by means of recurrence relations, and the pseudo-hydrodynamic flow and vorticity reconstructed.

One of the main aims of PMFB is to determine a scaling exponent that characterises the singularity in vorticity as the singular manifold is approached, introducing an exponent β with $\omega \sim s^{-\beta}$, where s is a coordinate perpendicular to the singular manifold. The exponent β is also linked to the scaling behaviour of high frequency Fourier modes in the original fluid mechanical problem: the exponential part of the fall-off gives information about the location of the singular manifold and $\delta_{\rm an}(t)$ while the power-law prefactor is linked to β. The problem in PMFB, with two complex modes, is characterised by two parameters, the angle ϕ between the modes, and the ratio of their wave numbers, η. The question posed by these authors is: how does the exponent β vary over this parameter set $\{\eta, \phi\}$? The results of the paper indicate that β is independent of η but does depend on ϕ, so for example $\beta \simeq 5/6$ for $\phi = \pi/2$. Having said this, there remains considerable uncertainty because of problems of slow convergence, which need to be speeded up by extrapolation methods, and the intensive, high precision numerical runs required for each value of the $\{\eta, \phi\}$ parameter space; for the most recent information see WP.

The aim of the present paper is to obtain information about the singular manifold and its scaling exponents using classical asymptotic methods that complement the approach of PMFB and related papers. We begin by reducing the problem posed in PMFB to an infinite hierarchy of ODEs in section 2. These are written in a variety of forms and are solved numerically to confirm the pseudo-hydrodynamic picture of PMFB. We find the same problem of slow convergence, and this prevents us from accurate determination of scaling exponents. Our ultimate aim is instead to pin these down by means of an asymptotic description of the vorticity along the singular manifold. For the present we are only been able to solve this in the limiting case when $\phi = 0$ and the two initial modes tend to be parallel. (There is also some rescaling of time taking place as the limit $\phi \to 0$ is taken, otherwise the initial condition is trivially a solution of the steady Euler equation.) The limit $\phi = 0$ is very attractive as determination of the exponent in WP leads to a value $\beta = 1$ (and similarly for $\phi = \pi$ the result $\beta = \frac{1}{2}$ is found). These results have been determined to a very high accuracy: the point here is that in these particular cases of $\phi = 0$ and π, asymptotic extrapolation methods can be used to determine not only β but also the next correction to the series for the scaling behaviour, which appears to emerge with a simple structure. The slow convergence observed for general angles ϕ including $\phi = \pi/2$, plus uncertainty as to the form of the next correction, make the exponents found in these cases much less precise.

We therefore focus on the parallel case: in section 3 with an appropriate *ansatz* for $\beta = 1$, we convert the limit of the infinite hierarchy of ODEs into a finite set of ODEs for functions δ, C_0 and A_0 that describe the shape of the singular manifold and the vorticity and stream function along it, valid for any angle ϕ. We then look at the far right-hand tail of the manifold, as a coordinate

$Y_1 \to \infty$, and exploit this to fix a number of constants that describe the limiting behaviour, using a uniformity assumption that we state in section 3.3. This fixes some of the structure of the vorticity and stream function in terms of the parameters $\{\eta, \phi\}$. The manifold however has two tails and a similar analysis can be undertaken for the left-hand tail. In section 4 we match up the two tails, to find that our initial assumption that $\beta = 1$ and the expansions used are only consistent with $\phi = 0$. This is in agreement with WP's result $\beta = 1$ for $\phi = 0$ and consistent with PMFB who find values of β that are smaller than unity for $\phi = \pi/4$ and $\pi/2$. For confirmation that our framework, that is the form of the asymptotic series and the uniformity assumption, is correct we develop exact solutions of the ODE hierarchy in section 5 with the help of computer algebra. This gives excellent agreement with our analytical development and confirms the *ansatz* used. Finally section 6 offers concluding discussion.

2 Reduction to a hierarchy of ODEs

In this section we develop theory starting with the Euler equation and derive infinite hierarchies of third order ODEs, whose asymptotic behaviour will describe the location and structure of the singular manifold. We break this up as follows: in section 2.1 we give the governing PDEs, and establish controlling parameters and symmetries. We aim to do this succinctly, and save background discussion and links to the study PMFB for the following section 2.2. Then in sections 2.3 and 2.4 we develop the two hierarchies of ODEs and present numerical solutions.

2.1 Euler equation and transformation to $\boldsymbol{Y}$-coordinates

Our starting point is the incompressible two-dimensional Euler equation written in the standard form

$$\partial_t \omega = J_{\boldsymbol{x}}(\psi, \omega), \quad -\omega = \nabla^2_{\boldsymbol{x}} \psi, \tag{2.1}$$

where $J_{\boldsymbol{x}}$ and $\nabla_{\boldsymbol{x}}$ are the Jacobian and gradient with respect to the (x_1, x_2) coordinates and the corresponding flow is

$$\boldsymbol{u} = (\partial_{x_2}\psi, -\partial_{x_1}\psi). \tag{2.2}$$

We now complexify, extending

$$x_1 \to z_1 = x_1 + iy_1, \quad x_2 \to z_2 = x_2 + iy_2, \tag{2.3}$$

and looking 'above' a fixed real point $\boldsymbol{x}$ as discussed further in section 2.2 below, we obtain the equations rewritten in terms of $\boldsymbol{y}$-variables by replacing

$$\partial_{x_1} = -i\partial_{y_1}, \quad \partial_{x_2} = -i\partial_{y_2}, \quad J_{\boldsymbol{x}} = -J_{\boldsymbol{y}}, \quad \nabla^2_{\boldsymbol{x}} = -\nabla^2_{\boldsymbol{y}}, \tag{2.4}$$

to give

$$\partial_t \omega = -J_{\boldsymbol{y}}(\psi, \omega), \quad \omega = \nabla^2_{\boldsymbol{y}} \psi. \tag{2.5}$$

We use the general two-mode initial condition

$$\psi|_{t=0} = ae^{\boldsymbol{p}\cdot\boldsymbol{y}} + be^{\boldsymbol{q}\cdot\boldsymbol{y}}, \quad \boldsymbol{p} \equiv p(\cos\phi_p, \sin\phi_p), \quad \boldsymbol{q} \equiv q(\cos\phi_q, \sin\phi_q), \tag{2.6}$$

with a and b assumed to be real (as can be achieved by a suitable choice of the fixed point $\boldsymbol{x}$). We require the modes to be non-parallel and unequal, specifying

$$p, q > 0, \quad p \neq q, \quad \sin\phi \neq 0, \quad \phi \equiv \phi_q - \phi_p, \tag{2.7}$$

otherwise the solution of (2.5) is steady and ininteresting.

The mathematical problem is to solve the PDEs (2.5) with the initial condition (2.6). This is specified by the parameter set $\{\boldsymbol{p}, \boldsymbol{q}, a, b\}$ and there is a natural relabelling symmetry of swapping the modes, which we denote by a bar, with

$$\{\bar{\boldsymbol{p}}, \bar{\boldsymbol{q}}, \bar{a}, \bar{b}, \bar{\psi}, \bar{\omega}\} = \{\boldsymbol{q}, \boldsymbol{p}, b, a, \psi, \omega\}. \tag{2.8}$$

We will be interested in the limit $t \to 0^+$ and make a transformation to real, positive $\boldsymbol{Y}$-variables given by the transformation

$$Y_1 = te^{\boldsymbol{p}\cdot\boldsymbol{y}}, \quad Y_2 = te^{\boldsymbol{q}\cdot\boldsymbol{y}}. \tag{2.9}$$

We set

$$\psi(y_1, y_2, t) = t^{-1}\Psi(Y_1, Y_2), \quad \omega(y_1, y_2, t) = t^{-1}\Omega(Y_1, Y_2). \tag{2.10}$$

In due course we will be interested in regions $\boldsymbol{Y} = O(1)$ as $t \to 0^+$. However we first proceed without approximation: the governing equations (2.5) become

$$(-1 + Y_1\partial_1 + Y_2\partial_2)\Omega = -pq\sin\phi\, Y_1Y_2[(\partial_1\Psi)(\partial_2\Omega) - (\partial_2\Psi)(\partial_1\Omega)], \tag{2.11}$$

$$\Omega = p^2Y_1\partial_1(Y_1\partial_1\Psi) + 2pq\cos\phi\, Y_1Y_2\partial_1\partial_2\Psi + q^2Y_2\partial_2(Y_2\partial_2\Psi), \tag{2.12}$$

with $\partial_1 \equiv \partial_{Y_1}$, $\partial_2 \equiv \partial_{Y_2}$. These are to be solved with the boundary condition

$$\Psi \sim aY_1 + bY_2 \qquad (Y_1, Y_2 \to 0). \tag{2.13}$$

Note that the original boundary condition (2.6) is applied for $t \to 0$ and $\boldsymbol{y}$ fixed whereas (2.13) is to be applied as $\boldsymbol{Y} \to 0$. The equations are parameterised now by $\{p, q, \phi, a, b\}$ and the relabelling symmetry (2.8) becomes

$$\{\bar{p}, \bar{q}, \bar{\phi}, \bar{a}, \bar{b}, \bar{Y}_1, \bar{Y}_2, \bar{\Psi}, \bar{\Omega}\} = \{q, p, -\phi, b, a, Y_2, Y_1, \Psi, \Omega\}. \tag{2.14}$$

We have exhibited the governing equations (2.11–2.13) with our initial parameter set so that their structure and the link with the Euler equation is evident: (2.11) is the vorticity equation while (2.12) is the vorticity–stream function relationship. However the number of parameters can be reduced from five to two (as pointed out in PMFB). Crucially for us, the factor $\sin\phi$ can be removed completely and so the limiting case $\phi = 0$ can be studied, this being the main subject of the present paper (see also WP). We will comment on this further shortly, but we now introduce a different scaling (reusing notation) in order to eliminate as many factors as possible. (Equations (2.9–2.13) will not be used again in the paper.)

First we recall that (a, b) are real, and we assume that

$$\operatorname{sign}\sin\phi = -\operatorname{sign} a = \operatorname{sign} b = \pm 1; \tag{2.15}$$

this can be arranged by an $\boldsymbol{x}$-translation. This choice of point $\boldsymbol{x}$ over which we are working will yield a singular manifold in the real region $\boldsymbol{Y} = O(1)$ as $t \to 0^+$. The new rescaling is

$$(-apqt\sin\phi)\, e^{\boldsymbol{p}\cdot\boldsymbol{y}} = Y_1, \quad (bpqt\sin\phi)\, e^{\boldsymbol{q}\cdot\boldsymbol{y}} = Y_2, \tag{2.16}$$

$$\psi(y_1, y_2, t) = (pqt\sin\phi)^{-1}\Psi(Y_1, Y_2), \quad \omega(y_1, y_2, t) = (t\sin\phi)^{-1}\Omega(Y_1, Y_2); \tag{2.17}$$

note that Y_1 and Y_2 are positive by virtue of (2.15). The resulting governing equations are

$$(-1 + Y_1\partial_1 + Y_2\partial_2)\Omega = -Y_1Y_2[(\partial_1\Psi)(\partial_2\Omega) - (\partial_2\Psi)(\partial_1\Omega)], \tag{2.18}$$

$$\Omega = \eta^{-1}Y_1\partial_1(Y_1\partial_1\Psi) + 2\cos\phi\, Y_1Y_2\partial_1\partial_2\Psi + \eta Y_2\partial_2(Y_2\partial_2\Psi), \tag{2.19}$$

with

$$\Psi \sim -Y_1 + Y_2 \qquad (Y_1, Y_2 \to 0) \tag{2.20}$$

and η defined as the ratio of wavenumbers of the modes,

$$\eta = q/p. \tag{2.21}$$

The rest of this paper concerns the solution of (2.18–2.20), parameterised only by $\{\eta, \phi\}$; the relabelling symmetry becomes

$$\{\bar\eta, \bar\phi, \bar Y_1, \bar Y_2, \bar\Psi, \bar\Omega\} = \{\eta^{-1}, -\phi, Y_2, Y_1, -\Psi, -\Omega\} \tag{2.22}$$

and we note that the factors of $\sin\phi$ in (2.17) have made Ψ and Ω pseudoscalars, which change sign under this interchange of axes.

2.2 Discussion and link to PMFB

Our study builds on that in PMFB, which should be consulted for more discussion: here we simply establish the connection and introduce some notation. These authors consider the 'standard orthogonal condition' (SOC) for the Euler equation (2.1),

$$\psi|_{t=0} = \cos px_1 + \cos qx_2, \tag{2.23}$$

with $p = 1$ and $q = 2$. This may be expressed in terms of complex coordinates via (2.3) and the $\boldsymbol{x}$-coordinates fixed to give the following initial condition,

$$\psi|_{t=0} = ae^{py_1} + be^{qy_2} + ce^{-py_1} + de^{-qy_2}, \tag{2.24}$$

with constants

$$a = \tfrac{1}{2}e^{-ipx_1}, \quad b = \tfrac{1}{2}e^{-iqx_2}, \quad c = \tfrac{1}{2}e^{ipx_1}, \quad d = \tfrac{1}{2}\ e^{iqx_2}. \tag{2.25}$$

We have four modes here, and adjacent pairs of modes can interact to give a singular manifold in the full space $\boldsymbol{z} = (z_1, z_2)$. For each pair a careful choice of the fixed point $\boldsymbol{x}$ allows the singular manifold to sit in the (real) $\boldsymbol{y}$-plane, at a distance of order $\log t^{-1}$ from the origin as $t \to 0^+$. These four manifolds will eventually interact as t increases, and must do non-trivially in order to obtain the full Euler flow dynamics in the original real domain. However our restricted aim in this paper is to study the manifold that arises from just two flow modes; so we set $c = d = 0$. With the choice of point $\boldsymbol{x} = (\pi, 0)$ we note the values (used by PMFB),

$$-a = b = \tfrac{1}{2}, \quad p = 1, \quad q = 2, \quad \eta = 2, \quad \phi = \pi/2 \qquad \text{(SOC)}. \tag{2.26}$$

Note that with these choices the conditions (2.15) above are satisfied.

PMFB apply a translation from $\boldsymbol{y}$- to $\tilde{\boldsymbol{y}}$-coordinates defined by

$$e^{\boldsymbol{p}\cdot\tilde{\boldsymbol{y}}} = te^{\boldsymbol{p}\cdot\boldsymbol{y}} = (-apq\sin\phi)^{-1}Y_1, \quad e^{\boldsymbol{q}\cdot\tilde{\boldsymbol{y}}} = te^{\boldsymbol{q}\cdot\boldsymbol{y}} = (bpq\sin\phi)^{-1}Y_2, \tag{2.27}$$

(using (2.16)). This translation is given by

$$\tilde{\boldsymbol{y}} = \boldsymbol{y} - \boldsymbol{\lambda}\log t^{-1}, \quad \boldsymbol{\lambda} = \boldsymbol{M}^{-1}(1,1)^{\mathrm{T}}, \tag{2.28}$$

where

$$\boldsymbol{M} = \begin{pmatrix} p\cos\phi_p & p\sin\phi_p \\ q\cos\phi_q & q\sin\phi_q \end{pmatrix}, \quad \boldsymbol{M}^{-1} = \frac{1}{pq\sin\phi}\begin{pmatrix} q\sin\phi_q & -p\sin\phi_p \\ -q\cos\phi_q & p\cos\phi_p \end{pmatrix}. \tag{2.29}$$

PMFB then define the pseudo-hydrodynamic stream function and vorticity by

$$\psi_{\mathrm{ps}} = \lambda_2\tilde{y}_1 - \lambda_1\tilde{y}_2 + t\psi, \quad \omega_{\mathrm{ps}} = -t\omega, \tag{2.30}$$

or, mapped into our notation,

$$\psi_{\rm ps} = (pq\sin\phi)^{-1}[\log(Y_1/Y_2) + \Psi + \log(-b/a)], \quad \omega_{\rm ps} = -(\sin\phi)^{-1}\Omega, \quad (2.31)$$

then, as discussed in PMFB, these quantities as functions of $\tilde{\boldsymbol{y}}$ satisfy equations for a steady fluid flow with Rayleigh friction,

$$\omega_{\rm ps} = J_{\tilde{\boldsymbol{y}}}(\psi_{\rm ps}, \omega_{\rm ps}), \quad \omega_{\rm ps} = -\nabla^2_{\tilde{\boldsymbol{y}}}\psi_{\rm ps}. \quad (2.32)$$

For our purposes the key point is that in the first of these equations, $\omega_{\rm ps}$ is propagated along characteristics of constant stream function $\psi_{\rm ps}$, and one such characteristic is the singular manifold itself. Note that if all the parameters $\{p, q, a, b, \phi\}$ at the outset are of order unity, then the singular manifold given by solving (2.18–2.20) will lie at $\boldsymbol{Y}$-coordinates of order unity: this translates into $\tilde{\boldsymbol{y}}$ of order unity and $\boldsymbol{y} = O(\log t^{-1})$ for small t, which of course motivates the approach of PMFB and this paper.

We will eventually focus on the limit $\phi \to 0$ in our analytical study: in this case we again obtain a singular manifold for $\boldsymbol{Y} = O(1)$. We note that the conversion back to $\boldsymbol{y}$-coordinates involves a small parameter ϕ, both in (2.27) and in the coordinate transformation matrix (2.29). To clarify these issues, take $-\phi_p = \phi_q = \phi/2$ for definiteness, so that we have at leading order as $\phi \to 0$,

$$\boldsymbol{y} \simeq \boldsymbol{M}^{-1}\begin{pmatrix} \log Y_1 + \log(-apqt\phi)^{-1} \\ \log Y_2 + \log(bptq\phi)^{-1} \end{pmatrix}, \quad \boldsymbol{M}^{-1} \simeq \frac{1}{2pq\phi}\begin{pmatrix} q\phi & p\phi \\ -2q & 2p \end{pmatrix}. \quad (2.33)$$

In conclusion, our rescaling (2.16,2.17) yields the system (2.18–2.20) which can sensibly solved with any ϕ including $\phi = 0$. For ϕ non-zero, the embedding of a singular manifold and associated quantities back in the $\boldsymbol{y}$-space is straightforward, involving a translation of order $\log t^{-1}$ together with a scaling of order unity. However as $\phi \to 0$, from (2.33) it may be seen that the singular manifold will occur at locations $y_1 = O(\log(t\phi)^{-1})$ and $y_2 = O(\phi^{-1}\log(t\phi)^{-1})$. The factor of ϕ^{-1} in $\boldsymbol{M}$ in (2.33) also means that the solution becomes increasingly stretched in the y_2-direction as $\phi \to 0$.

2.3 First hierarchy of ODEs

So far we have just established notation and given discussion that parallels PMFB and WP. We now consider solving (2.18–2.20), for any ϕ. One option is an expansion in powers $Y_1^m Y_2^n$; this gives the two-dimensional, exact recurrence relation studied in PMFB for powers $m, n \geq 0$ up to values of order 1000, using high precision arithmetic.

We take a different approach, by expanding to give a recurrence relation in one direction only. We expand in powers of Y_2 with

$$\Psi = f_0(Y_1)+f_1(Y_1)Y_2+f_2(Y_1)Y_2^2+\cdots, \quad \Omega = h_0(Y_1)+h_1(Y_1)Y_2+h_2(Y_1)Y_2^2+\cdots. \tag{2.34}$$

Of course we could equally well expand in powers of Y_1, but more conveniently we can at any time use the symmetry (2.22) to exchange the coordinates. With this substitution the PDEs (2.18,2.19) yield a hierarchy of ODEs in Y_1, labelled by n. We can consider the solutions of these ODEs and obtain them numerically, for the whole range of $Y_1 \in [0,\infty)$. However we are restricted to moderate values of n; for this reason will refer to this as an expansion along the 'edge region'. We note in passing that PMFB also focus on these edge regions in their §3.4.

The expansions (2.34) are substituted into (2.18–2.20) and powers of Y_2 are equated. At leading order Y_2^0, the equations and initial conditions give the exact solution for parallel shear flow, namely

$$f_0(Y_1) \equiv -Y_1, \quad h_0(Y_1) \equiv -\eta^{-1}Y_1. \tag{2.35}$$

For further orders $n \geq 1$ we obtain the following hierarchy of linear, third order systems,

$$Y_1 h_n' + (n-1)h_n - nY_1(h_n - \eta^{-1}f_n) = -s_n, \tag{2.36}$$
$$g_n = Y_1 f_n', \tag{2.37}$$
$$h_n = \eta^{-1}Y_1 g_n' + 2n\cos\phi\, g_n + \eta n^2 f_n, \tag{2.38}$$

each driven by lower members according to the quadratic source term,

$$s_n = \sum_{r=1}^{n-1} Y_1[(n-r)f_r' h_{n-r} - r f_r h_{n-r}']. \tag{2.39}$$

Note that we have moved the interactions of mode n with mode 0 in (2.35) to the left-hand side of (2.36); these would otherwise appear in s_n for $r = 0$ and $r = n$. From (2.20) the initial conditions, at $Y_1 = 0$, are

$$f_1 = 1, \quad h_1 = \eta, \quad f_n = h_n = 0 \qquad (n \geq 2). \tag{2.40}$$

We call this the $\{f_n, h_n\}$ hierarchy, and while we have introduced g_n for convenience (in particular when the equations become more complicated below), in our discussion we largely ignore g_n and focus on the f_n stream function modes and the h_n vorticity modes.

If in (2.36–2.38) s_n is set to zero, the resulting homogeneous equations have solutions of Frobenius form for small Y_1, first a solution

$$f_n \sim Y_1^{1-n}, \quad h_n \sim [\eta^{-1}(1-n)^2 + 2n(1-n)\cos\phi + \eta n^2]Y_1^{1-n}, \tag{2.41}$$

and then two that are generally oscillatory

$$f_n \sim Y_1^{\mu_\pm}, \quad h_n \sim -\eta^{-1} n(n+\mu_\pm)^{-1} Y_1^{\mu_\pm+1}, \quad \mu_\pm \equiv -\eta n e^{\pm i\phi}, \tag{2.42}$$

for small Y_1. These solutions all continue as series in powers of Y_1, and corrections can be written as a multiplying factor of $1 + O(Y_1)$.

Clearly (2.41) ties up with the initial conditions in (2.40) for $n = 1$: for $n \geq 2$ (2.40) is to be interpreted as excluding solutions of the form (2.41) (which would correspond to modes $e^{i(n-1)\boldsymbol{p}\cdot\boldsymbol{x}+in\boldsymbol{q}\cdot\boldsymbol{x}}$, absent from the initial conditions). In fact, as is clear from the hierarchy of recurrence relations in PMFB, for the given two-mode initial condition (2.20) the quantities f_n and h_n are required to expand in positive powers of Y_1 as $Y_1 \to 0$ for $n \geq 2$, and non-negative powers in the case $n = 1$; in particular

$$f_1 \sim 1, \quad h_1 \sim \eta, \quad f_n, h_n = O(Y_1) \qquad (n \geq 2). \tag{2.43}$$

For general values of the angle ϕ we must therefore exclude solutions with the oscillatory form (2.42); for $\phi = 0$ the roots $\mu_\pm$ are repeated and a similar solution growing as $Y_1^{-\eta n}$ is to be excluded, together with one involving a logarithm (see section 5). Finally the limiting case $\phi = \pi$ is special as the solution $Y_1^{\eta n}$ in (2.42) is admissible for integer η; this corresponds to the non-trivial solution $f_n = Y_1^{\eta n}$, $h_n = 0$ for irrotational flow in (2.38). We will not consider the limiting case $\phi = \pi$ in this paper but note that the paper WP discusses its problematic behaviour further.

To give a feeling for these functions, figure 1(a,b) shows solutions of the hierarchy of equations (2.36–2.40) for $n = 1$ to 10. As Y_1 increases, the initial power law behaviour is taken over by exponential growth, seen as asymptotically straight lines in figure 1(c,d); this growth is increasingly rapid as n increases, enabling the reader to distinguish the different values of n in the figure.

2.4 Second hierarchy of ODEs

It clearly makes sense to pull out the exponential growth evident in figure 1 for large Y_1. Setting s_n to zero again, each homogeneous third order system (2.36–2.38) has solutions with the following behaviour as $Y_1 \to \infty$,

$$f_n \sim e^{nY_1} Y_1^{-n-1}, \quad h_n \sim \eta^{-1} n^2 e^{nY_1} Y_1^{-n+1}, \tag{2.44}$$

$$f_n \sim Y_1^{\nu_\pm}, \quad h_n \sim \eta^{-1} Y_1^{\nu_\pm}, \quad \nu_\pm \equiv -\eta n \cos\phi \pm \sqrt{1 - \eta^2 n^2 \sin^2\phi}\,. \tag{2.45}$$

These solutions all continue in powers of Y_1^{-1}. Of these solutions the first is dominant as $Y_1 \to \infty$ for all parameter values.

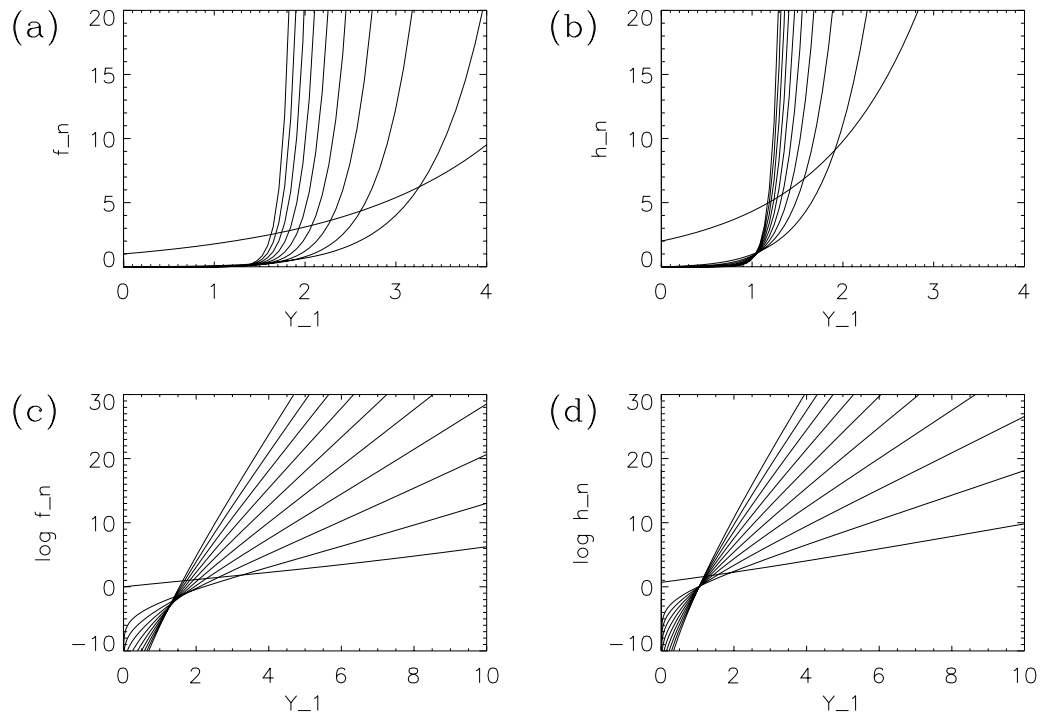

Fig. 1. Plotted in (a) are the stream function modes f_n and in (b) the vorticity modes h_n, against Y_1 for $n = 1$ up to $n = 10$ and $\eta = 2$, $\phi = \pi/2$. In (c) and (d) we show $\log f_n$ and $\log h_n$ respectively.

Reintroducing the coupling s_n between each mode and lower members of the hierarchy, if we fix n and increase Y_1, the far-field solution for (f_n, h_n) could be controlled either by the homogeneous solution (2.44) or by the forced component, the linear response to s_n. It turns out it is the homogeneous component that dominates in the far-field solution: informally the nonlinear interactions switch off at leading order in the tail of the manifold. This consideration, which is easily checked *a posteriori*, motivates the change of variables

$$f_n(Y_1) = e^{nY_1} Y_1^{-n-1} F_n(Y_1), \quad g_n(Y_1) = e^{nY_1} Y_1^{-n} G_n(Y_1), \quad h_n(Y_1) = e^{nY_1} Y_1^{-n+1} H_n(Y_1), \tag{2.46}$$

to give what we refer to as the $\{F_n, H_n\}$ hierarchy,

$$Y_1^2 H_n' + \eta^{-1} n F_n = -S_n, \tag{2.47}$$
$$Y_1 G_n = Y_1 F_n' + (nY_1 - n - 1) F_n, \tag{2.48}$$
$$Y_1 H_n = \eta^{-1}[Y_1 G_n' + (nY_1 - n) G_n] + 2n \cos\phi \, G_n + \eta n^2 Y_1^{-1} F_n, \tag{2.49}$$

with

$$S_n = \sum_{r=1}^{n-1} [(n-r) Y_1 F_r' H_{n-r} - r Y_1 F_r H_{n-r}' - n F_r H_{n-r}], \tag{2.50}$$

and the initial conditions as $Y_1 \to 0$,

$$F_1 = 0, \quad G_1 = 0, \quad H_1 = \eta, \quad F_n = G_n = H_n = 0 \qquad (n \geq 2). \tag{2.51}$$

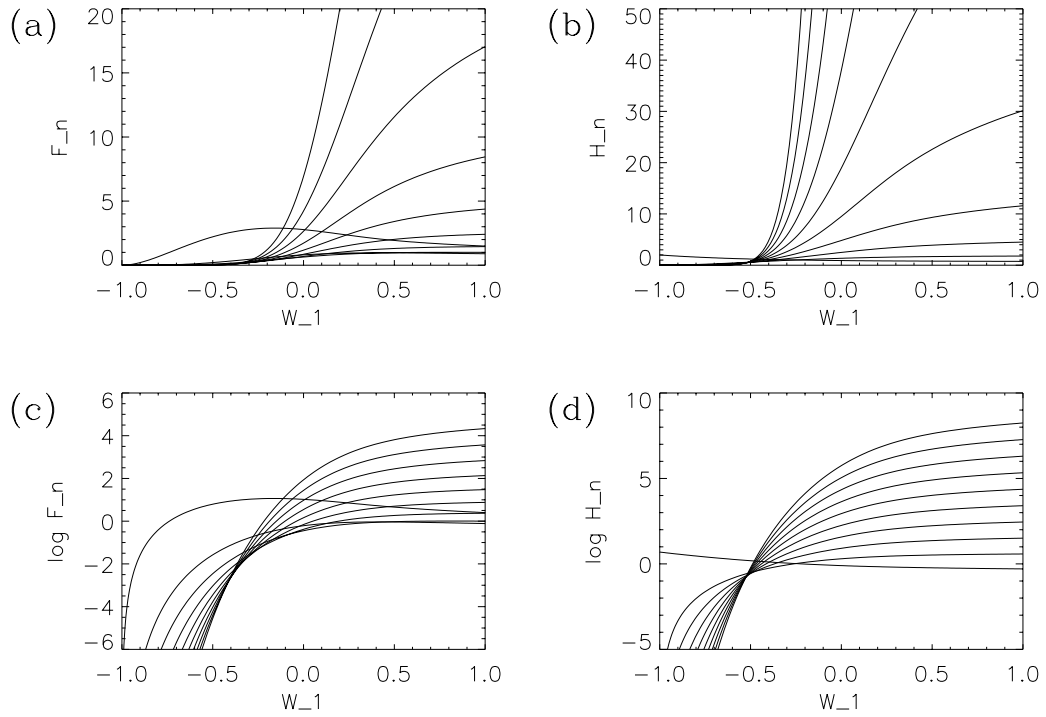

Fig. 2. Plotted in (a) are the stream function modes F_n and in (b) the vorticity modes H_n, against W_1 for $n = 1$ up to $n = 10$ and $\eta = 2$, $\phi = \pi/2$. In (c) and (d) we show $\log F_n$ and $\log H_n$ respectively.

More precisely, from (2.40) we require

$$F_1 \sim Y_1^2, \quad H_1 \sim \eta, \quad F_n = O(Y_1^{n+2}), \quad H_n = O(Y_1^n) \qquad (n \geq 2). \tag{2.52}$$

as $Y_1 \to 0$.

The $\{F_n, H_n\}$ hierarchy is attractive since solutions expand in powers of Y_1 as $Y_1 \to 0$ and powers of Y_1^{-1} as $Y_1 \to \infty$. The functions tend to constants as $Y_1 \to \infty$; as n increases the functions also become increasingly flat near the origin. Figure 2 shows the functions F_n and H_n, together with their logarithms. Here we have changed independent variable from $Y_1 \in [0, \infty)$ to $W_1 \in [-1, 1]$ with the choice

$$Y_1 = \mu \frac{W_1 + 1}{4 - (W_1 + 1)^2}, \quad \frac{dY_1}{dW_1} = \mu \frac{4 + (W_1 + 1_)^2}{(4 - (W_1 + 1)^2)^2}, \quad \mu = 20. \tag{2.53}$$

This coordinate change is chosen so that the functions F_n, H_n expand in powers of $W_1 + 1$ and $W_1 - 1$ at the two endpoints. The change allows the solution of the ODEs by time-stepping or by collocation methods, all the way to $W_1 = 1$; as this corresponds to the limit $Y_1 \to \infty$ we have, in some sense, conquered the edge region, at least for modest values of n in the hierarchy.

Figures 1–6 were obtained by expressing the functions in terms of N Cheby-

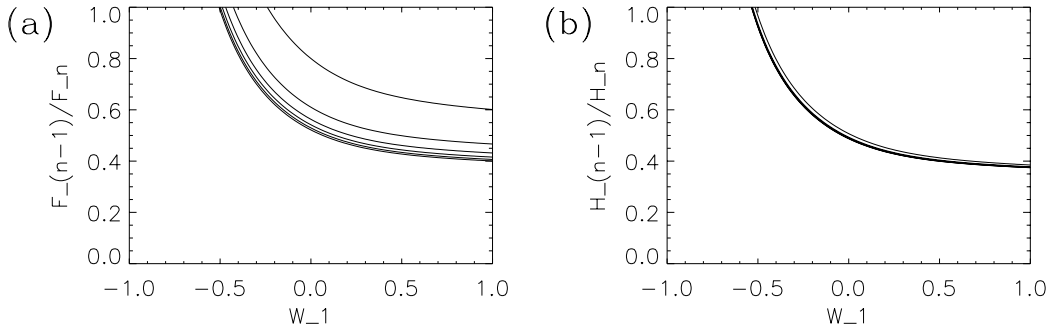

Fig. 3. Plotted are the ratios (a) F_{n-1}/F_n and (b) H_{n-1}/H_n against W_1 for $n = 5$, 10, $15 \ldots, 30$, with $\eta = 2$ and $\phi = \pi/2$. These accumulate on the function $\Delta(Y_1)$.

chev polynomials

$$F_n \simeq \sum_{m=0}^{N-1} a_{n,m} T_m(W_1), \quad G_n \simeq \sum_{m=0}^{N-1} b_{n,m} T_m(W_1), \quad H_n \simeq \sum_{m=0}^{N-1} c_{n,m} T_m(W_1). \tag{2.54}$$

For each n, the linear equations (2.47–2.49) are imposed at N standard collocation points (zeros of $T_N(W_1)$) as $3N$ rows of a $(3N+3)^2$ matrix, with the quadratic forcing (2.50) also evaluated at the collocation points. The remaining three rows impose boundary conditions (2.51) on F_n, G_n and H_n at $W_1 = -1$. Note that this scheme has a number of advantages over stepping in Y_1 from $Y_1 = 0$: each linear third order system in the hierarchy is integrated separately, and the coefficients of the differential equation are never evaluated where they are singular, that is at $Y_1 = 0$ or ∞, $W_1 = \pm 1$.

In figure 2 we observe the saturation of F_n and H_n to constant levels as $Y_1 \to \infty$ or $W_1 \to 1$ as expected, and we can also see, in figure 2(c,d), that these functions have approximately constant ratios for each Y_1 and large n. To quantify this, we define the function

$$\Delta(Y_1) = \lim_{n\to\infty} F_{n-1}(Y_1)/F_n(Y_1) = \lim_{n\to\infty} H_{n-1}(Y_1)/H_n(Y_1), \tag{2.55}$$

Figure 3 shows approximations to this limit, plotted as functions of W_1 for $n = 5,\ 10, \ldots, 30$. It may be seen that the function $\Delta(Y_1)$ converges very rapidly for the H_n ratios (most curves overlap) and well also for the F_n ratios.

The function $\Delta(Y_1)$ determines the radius of convergence of the series expansion (2.34) as Y_2 is increased for fixed Y_1. If we define a new coordinate by

$$W_2 \equiv Y_2 Y_1^{-1} e^{Y_1}, \tag{2.56}$$

then in view of (2.46) the radius of convergence is given by

$$W_2 = \Delta(Y_1). \tag{2.57}$$

This also marks the location of the singular manifold as we find numerically

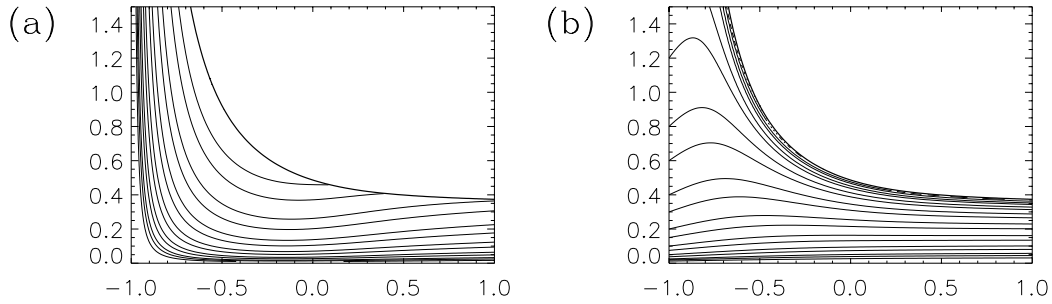

Fig. 4. Panel (a) depicts $\mathcal{F}$ and (b) $\mathcal{H}$, as contour plots in the (W_1, W_2)-plane, reconstructed for the SOC case (2.26) using $n = 40$ modes, with $\eta = 2$ and $\phi = \pi/2$. Contours lie at 0.025×2^j, 0.0375×2^j for $j = 0, 1, \ldots, 10$. The singular manifold is the bounding, bold curve.

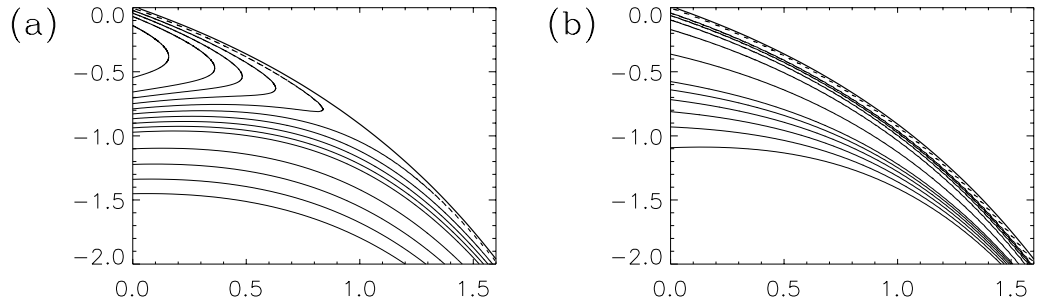

Fig. 5. Plotted in (a) is $\psi_{\rm ps}$ and in (b) $\omega_{\rm ps}$, as functions of $(\tilde{y}_1, \tilde{y}_2)$ reconstructed using $n = 40$ modes with contour levels as in PMFB.

that the functions F_n and H_n are everywhere positive (as discussed in more detail in PMFB). Thus figure 3 depicts the location of the singular manifold in the real (W_1, W_2)-plane.

We can also write the series (2.34) in the form

$$\Psi = Y_1^{-1}[-Y_1^2 + \mathcal{F}(Y_1, W_2)], \tag{2.58}$$
$$\Omega = Y_1[-\eta^{-1} + \mathcal{H}(Y_1, W_2)], \tag{2.59}$$

with

$$\mathcal{F}(Y_1, W_2) = W_2 F_1(Y_1) + W_2^2 F_2(Y_1) + \cdots, \tag{2.60}$$
$$\mathcal{H}(Y_1, W_2) = W_2 H_1(Y_1) + W_2^2 H_2(Y_1) + \cdots, \tag{2.61}$$

and the pseudo-hydrodynamic stream function in (2.31) is given by

$$\psi_{\rm ps} = (pq \sin\phi)^{-1}[-\log W_2 + Y_1^{-1}\mathcal{F}(Y_1, W_2) + \log(-b/a)]. \tag{2.62}$$

To illustrate this, we show $\mathcal{F}$ and $\mathcal{H}$ as contour plots in the (W_1, W_2)-plane in figure 4(a,b). We use $n = 40$ modes, which is enough to obtain the pictures to graphical accuracy. It is not however enough to ascertain the scaling behaviour

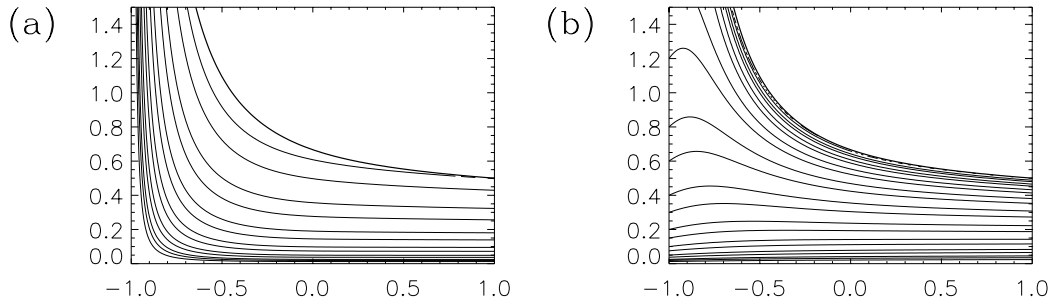

Fig. 6. As for panels (a,b) of figure 4 but for $\eta = 2$ in the parallel case $\phi = 0$.

near the singular manifold, and from this point of view our numerical methods are inferior to those in PMFB. To tie our results more closely to this study and as a check we also plot the pseudo-hydrodynamic stream function and vorticity in figure5(a,b), which may be compared with figure 14 of PMFB. The vorticity $\omega_{\rm ps}$ diverges on the bounding curve, the singular manifold, whereas $\psi_{\rm ps}$ has a finite limit there.

We are unable to study asymptotically the case $\phi = \pi/2$ that is the focus of PMFB, and below we will consider $\phi = 0$. We show in figure 6 the functions $\mathcal{F}$ and $\mathcal{H}$ reconstructed in this case. These show a similar overall form. The scaling laws for vorticity as the singular manifold is approached are different, as we now outline.

3 Asymptotic structure of manifolds for $\phi = 0$

3.1 Preamble

So far we have not approximated anything, merely expanded in various ways. In fact our work is still very closely linked to PMFB, in that the Taylor series coefficients of the functions f_n, h_n give the coefficients studied there in the edge regions (as in their section 3.4). Our aim now is to push our understanding by means of asymptotic expansions of the hierarchy of ODEs, focussing on the $\{F_n, H_n\}$ formulation in equations (2.47–2.50), and working with an expansion of the form,

$$F_n = n^{-\alpha(Y_1)-2} e^{-n\delta(Y_1)}(A_0(Y_1) + \cdots), \quad H_n = n^{-\alpha(Y_1)} e^{-n\delta(Y_1)}(C_0(Y_1) + \cdots). \tag{3.1}$$

Here α is the singularity exponent and we describe A_0 and C_0 as the stream function and vorticity 'prefactors'. In view of (2.55), the decrement $\delta(Y_1)$ gives the location of the singular manifold,

$$W_2 \equiv Y_2 Y_1^{-1} e^{Y_1} = \Delta(Y_1) \equiv e^{\delta(Y_1)}. \tag{3.2}$$

The exponent α is shown to be constant, independent of Y_1, by PMFB. It is linked to the blow-up of vorticity on the singular manifold, with a power law of $(W_2 - \Delta(Y_1))^{-\beta}$ where $\beta = 1 - \alpha$. PMFB adopt slightly different conventions, placing their exponent α_{PMFB} on large wavenumber behaviour of stream function Fourier components (in two dimensions). These exponents are linked by

$$\alpha = 1 - \beta, \quad \alpha_{\mathrm{PMFB}} = 5/2 + \alpha = 7/2 - \beta. \tag{3.3}$$

We note the results of previous papers,

$$\phi = \pi/2, \quad \alpha_{\mathrm{PMFB}} \simeq 8/3, \quad \beta \simeq 5/6, \quad \alpha \simeq 1/6, \tag{3.4}$$
$$\phi = \pi/4, \quad \alpha_{\mathrm{PMFB}} \simeq 2.54, \quad \beta \simeq 0.96, \quad \alpha \simeq 0.04, \tag{3.5}$$
$$\phi = 0, \quad \alpha_{\mathrm{PMFB}} \simeq 5/2, \quad \beta \simeq 1, \quad \alpha \simeq 0, \tag{3.6}$$
$$\phi = \pi, \quad \alpha_{\mathrm{PMFB}} \simeq 3, \quad \beta \simeq 1/2, \quad \alpha \simeq 1/2. \tag{3.7}$$

The first two are from PMFB, obtained by extrapolation of large wavenumber scalings along lines in Fourier space, using their recurrence relations. The last pair are obtained in WP, and are established to high accuracy (with errors of no more than 10^{-7}) using asymptotic approximation techniques which permit the identification of not only the leading asymptotic terms in series similar to (3.1) but also the leading corrections.

Unfortunately we are not able to deal with the case of general α at present and the following analysis is limited to $\alpha = 0$, in which case the picture simplifies in a number of key aspects. We will leave ϕ in as a general parameter while we develop our asymptotic framework, but will eventually show that the picture with $\alpha = 0$ and an additional *uniformity assumption* is only consistent with $\phi = 0$.

3.2 Asymptotic limits

Having in mind the expansion (3.1) with $\alpha = 0$ we first set

$$F_n = n^{-2} e^{-n\delta(Y_1)} \hat{F}_n(Y_1), \tag{3.8}$$
$$G_n = n^{-1} e^{-n\delta(Y_1)} \hat{G}_n(Y_1), \tag{3.9}$$
$$H_n = e^{-n\delta(Y_1)} \hat{H}_n(Y_1), \tag{3.10}$$
$$S_n = n e^{-n\delta(Y_1)} \hat{S}_n(Y_1), \tag{3.11}$$

to obtain the equations that follow. These are exact and involve an extra function $\delta(Y_1)$ which we have not specified; when we require $\hat{F}_n$, $\hat{H}_n$ to be of

order unity as $n \to \infty$ it will be fixed, but at present it is arbitrary:

$$Y_1^2(-\delta'\hat{H}_n + n^{-1}\hat{H}'_n) + \eta^{-1}n^{-2}\hat{F}_n = -\hat{S}_n, \tag{3.12}$$

$$Y_1\hat{G}_n = Y_1(-\delta'\hat{F}_n + n^{-1}\hat{F}'_n) + (Y_1 - 1 - n^{-1})\hat{F}_n, \tag{3.13}$$

$$Y_1\hat{H}_n = \eta^{-1}[Y_1(-\delta'\hat{G}_n + n^{-1}\hat{G}'_n) + (Y_1 - 1)\hat{G}_n] + 2\cos\phi\,\hat{G}_n + \eta Y_1^{-1}\hat{F}_n, \tag{3.14}$$

$$\hat{S}_n = \sum_{r=1}^{n-1}\left[\frac{1}{r^2}\left(1 - \frac{r}{n}\right)Y_1\hat{F}'_r\hat{H}_{n-r} - \frac{1}{nr}\,Y_1\hat{F}_r\hat{H}'_{n-r} - \frac{1}{r^2}\,\hat{F}_r\hat{H}_{n-r}\right]. \tag{3.15}$$

Only now do we start to approximate. We assume certain expansions and try to build a consistent asymptotic picture. We do not prove that these expansions are the only possible ones, nor do we establish rigorously that they work to all orders; instead we take a pragmatic approach, to be tested in section 5 by explicit solutions obtained using Maple. We assume that in the limit $n \to \infty$,

$$\hat{F}_n(Y_1) \sim A_0(Y_1) + A_1(Y_1)n^{-1} + A_2(Y_1)n^{-2} + \cdots, \tag{3.16}$$

$$\hat{G}_n(Y_1) \sim B_0(Y_1) + B_1(Y_1)n^{-1} + B_2(Y_1)n^{-2} + \cdots, \tag{3.17}$$

$$\hat{H}_n(Y_1) \sim C_0(Y_1) + C_1(Y_1)n^{-1} + C_2(Y_1)n^{-2} + \cdots. \tag{3.18}$$

It is important to appreciate that these series expansions only become correct in the limit of large n. In particular the functions $\hat{F}_1$, $\hat{F}_2$, etc., for example, cannot in any sense be approximated by a combination of the terms A_0, A_1, etc., as the series will only generally be asymptotic and not convergent. We can refer to leading terms as the 'head' of the series, that is $\{\hat{F}_n\}$ for $n = O(1)$ and we refer to $\{\hat{F}_n\}$ for $n \gg 1$ as the 'tail' of the series. Note that only quantities that depend on the tails of the series can be expected to give general results for scaling exponents.

Recall that (3.12, 3.15) correspond to the vorticity equation, with the quadratic forcing of each linear $(\hat{F}_n, \hat{H}_n)$ system by lower orders of the hierarchy. We focus on the behaviour of this forcing term, namely $\hat{S}_n$ in (3.15), as $n \to \infty$. It is the leading terms $r = O(1)$ that dominate in the first and third sums (because of the fall-off in the sums); the second sum can be neglected. In fact we can legitimately approximate $\hat{H}_{n-r} \sim C_0$ for $r \ll n$ to leave the leading behaviour as

$$\hat{S}_n \sim \sum_{r=1}^{n-1} r^{-2}(Y_1\hat{F}'_r - \hat{F}_r)C_0 \qquad (n \to \infty). \tag{3.19}$$

(Of course we cannot approximate $\hat{F}_r$ as this involves the head of the series.) It is also consistent to write

$$\hat{S}_n \sim \hat{S}_n^{(0)} \equiv \sum_{r=1}^{\infty} r^{-2}(Y_1\hat{F}'_r - \hat{F}_r)\hat{H}_n \qquad (n \to \infty). \tag{3.20}$$

Corrections are of order $n^{-1}\log n$, as we shall see shortly. We combine this

with equations (3.12) and (3.15) to leave,

$$\Big[-Y_1^2\delta' + \sum_{r=1}^{\infty} r^{-2}(Y_1\hat{F}_r' - \hat{F}_r)\Big]\hat{H}_n + n^{-1}Y_1^2\hat{H}_n' + \eta^{-1}n^{-2}\hat{F}_n = -(\hat{S}_n - \hat{S}_n^{(0)}), \tag{3.21}$$

with

$$\begin{aligned}\hat{S}_n - \hat{S}_n^{(0)} = &-\sum_{r=1}^{n-1}\frac{1}{nr}\,Y_1(\hat{F}_r\hat{H}_{n-r})' + \sum_{r=1}^{n-1}\frac{1}{r^2}\,(Y_1\hat{F}_r' - \hat{F}_r)(\hat{H}_{n-r} - \hat{H}_n)\\ &- \sum_{r=n}^{\infty}\frac{1}{r^2}\,(Y_1\hat{F}_r' - \hat{F}_r)\hat{H}_n \equiv -\hat{S}_n^{\mathrm{I}} + \hat{S}_n^{\mathrm{II}} - \hat{S}_n^{\mathrm{III}}.\end{aligned} \tag{3.22}$$

We have in (3.22) three sums labelled $\hat{S}_n^{\mathrm{I}}$, $\hat{S}_n^{\mathrm{II}}$ and $\hat{S}_n^{\mathrm{III}}$ that contribute to the nonlinear forcing of higher harmonics by lower ones, and which go to zero as n tends to infinity: we will specify exactly how, shortly. Thus, for large n for equation (3.21) to make sense at leading order we require that

$$Y_1^2\delta' = \sum_{r=1}^{\infty} r^{-2}(Y_1\hat{F}_r' - \hat{F}_r). \tag{3.23}$$

The equation can be integrated once, giving

$$\delta = Y_1^{-1}\sum_{r=1}^{\infty} r^{-2}\hat{F}_r + \text{const.} \tag{3.24}$$

In view of (3.2, 3.8, 2.60) this can be written as

$$\log\Delta = Y_1^{-1}\sum_{r=1}^{\infty} F_r\Delta^r + \text{const.} = Y_1^{-1}\mathcal{F}(Y_1,\Delta) + \text{const.} \tag{3.25}$$

Unsurprisingly, but reassuringly, this gives conservation of the pseudo-hydrodynamic stream function on the singular manifold $W_2 = \Delta(Y_1)$; see (2.62).

3.3 Nonlinear driving through quadratic interactions

We now proceed to higher order, and need to know the leading order behaviours of the (unapproximated) sums left in (3.22). If we substitute possible components of the tail expansions (3.16–3.18) into $\hat{S}_n^{\mathrm{I}}$ and $\hat{S}_n^{\mathrm{II}}$ we find we need to evaluate sums of the following general form,

$$\Sigma_{P,Q} = \sum_{r=1}^{n-1} r^{-P}(n-r)^{-Q} \qquad (P,Q \geq 0), \tag{3.26}$$

for integers P and Q. These have the following scaling behaviour as $n \to \infty$,

$$\Sigma_{P,Q} \equiv \Sigma_{Q,P} = \begin{cases} n-1 & (P,Q) = 0, \\ O(\log n) & (P,Q) = (1,0), (0,1), \\ O(n^{-1}\log n) & (P,Q) = (1,1), \\ O(n^{-\min(P,Q)}) & \text{otherwise.} \end{cases} \tag{3.27}$$

Note that a limited number of logarithmic terms appear; these are crucial to the development. We will need the specific cases,

$$\Sigma_{1,0} = \log n + \gamma_{\mathrm{E}} - \tfrac{1}{2}n^{-1} + O(n^{-2}), \tag{3.28}$$
$$\Sigma_{1,1} = 2n^{-1}\log n + 2\gamma_{\mathrm{E}} n^{-1} + O(n^{-2}), \tag{3.29}$$

where γ_{E} is the Euler–Mascheroni constant. Using these, we may now approximate the sums in (3.22) as

$$\begin{aligned} \hat{S}_n^{\mathrm{I}} &= (n^{-1}\log n + \gamma_{\mathrm{E}} n^{-1}) Y_1 (A_0 C_0)' + n^{-1} \sum_{r=1}^{\infty} r^{-1} Y_1 [(\hat{F}_r - A_0) C_0]' \\ &\quad + 2n^{-2}\log n\, Y_1 (A_0 C_1)' + O(n^{-2}), \end{aligned} \tag{3.30}$$
$$\hat{S}_n^{\mathrm{II}} = 2n^{-2}\log n\, (Y_1 A_0' - A_0) C_1 + O(n^{-2}), \tag{3.31}$$
$$\hat{S}_n^{\mathrm{III}} = n^{-1}(Y_1 A_0' - A_0) C_0 + O(n^{-2}). \tag{3.32}$$

We give detailed justification in appendix A: here we note that at some orders we can approximate using just the tails of the series A_j, C_j whereas at others we need to retain the heads, and so $\hat{F}_r$ appears in $\hat{S}_n^{\mathrm{I}}$ above.

We now substitute the expansions (3.30–3.32), together with (3.16–3.18), into the vorticity equation (3.21, 3.22), to obtain a series of equations in decreasing orders of n as $n \to \infty$. We have at orders $n^{-1}\log n$, n^{-1} and $n^{-2}\log n$ respectively,

$$0 = Y_1 (A_0 C_0)', \tag{3.33}$$
$$Y_1^2 C_0' = \gamma_{\mathrm{E}} Y_1 (A_0 C_0)' + \sum_{r=1}^{\infty} r^{-1} Y_1 [(\hat{F}_r - A_0) C_0]' + (Y_1 A_0' - A_0) C_0, \tag{3.34}$$
$$0 = 2Y_1 (A_0 C_1)' - 2(Y_1 A_0' - A_0) C_1. \tag{3.35}$$

Note that instead of having zero on the left-hand side of equations (3.33, 3.35) one could instead contemplate introducing extra terms in the series (3.18), of magnitude $\log n$ and $n^{-1}\log n$ respectively. However the quadratic sums (3.26) then have to be supplemented by sums involving logarithms. Such sums have a more complicated form and then introduce further functions including squares of logarithms into our expansions, as discussed briefly in appendix A. Although we cannot rule this out on purely analytical grounds, it seems unlikely, and so we proceed pragmatically as above and check our results independently in section 5

We also have the vorticity–stream function relationship (3.13, 3.14). Substituting the series expansions (3.16–3.18) into (3.13) yields at leading orders

$$Y_1 B_0 = (-Y_1\delta' + Y_1 - 1)A_0, \tag{3.36}$$
$$Y_1 B_1 = (-Y_1\delta' + Y_1 - 1)A_1 + Y_1 A_0' - A_0, \tag{3.37}$$

and into (3.14) gives

$$Y_1 C_0 = \eta^{-1}(-Y_1\delta' + Y_1 - 1)B_0 + 2\cos\phi\, B_0 + \eta Y_1^{-1} A_0, \tag{3.38}$$
$$Y_1 C_1 = \eta^{-1}[(-Y_1\delta' + Y_1 - 1)B_1 + Y_1 B_0'] + 2\cos\phi\, B_1 + \eta Y_1^{-1} A_1. \tag{3.39}$$

Combining (3.36) and (3.38) gives

$$C_0 = LA_0, \tag{3.40}$$

where we define for convenience the function L,

$$L(Y_1) = Y_1^{-2}[\eta^{-1}(-Y_1\delta' + Y_1 - 1)^2 + 2\cos\phi\,(-Y_1\delta' + Y_1 - 1) + \eta] \geq 0, \tag{3.41}$$

and we recall that δ is linked to the shape of the singular manifold via (3.24). This factor L links vorticity and stream function and is in a sense the key simplification of our asymptotic expansion: the link through the Laplacian becomes purely a multiplicative factor L rather than a second order differential equation.

We now explore the consequences of these equations; the obvious immediate result is that, from (3.33),

$$A_0 C_0 = K_0^2 = \text{const.} \tag{3.42}$$

Here K_0 is a real constant and the form is chosen for convenience: C_0 and A_0 have the same sign since $L \geq 0$ from (3.41). We then have from (3.40) that

$$A_0 = K_0 L^{-1/2}, \quad C_0 = K_0 L^{1/2}. \tag{3.43}$$

These give information about the variation of the singularity prefactors A_0 and C_0 along the singular manifold as a function purely of its shape, given by $\delta(Y_1)$ and incorporated in L through (3.41).

To make further progress we need to assume certain expansions as $Y_1 \to \infty$. The functions $\hat{F}_n$, $\hat{H}_n$ have the property of expanding in inverse powers of Y_1 for given, fixed n, as Y_1 tends to infinity (see (2.44) and below). We make a **uniformity assumption** that other functions that appear asymptotically in the limit $n \to \infty$ expand in the same way. This assumption, which probably would need to be relaxed or modified in the case of non-zero α, allows us to construct a consistent asymptotic framework, which we verify in section 5. In short, we make the working hypothesis that there is uniform convergence in

dealing with the double limit $n \to \infty$ and $Y_1 \to \infty$. Quantities such as δ or A_0 then expand as

$$\delta(Y_1) = \delta_0 + \delta_1 Y_1^{-1} + \cdots, \qquad A_0(Y_1) = A_{00} + A_{01} Y_1^{-1} + \cdots, \tag{3.44}$$

in terms of constant coefficients δ_j or A_{0j}. We assume similar expansions for L and for any function C_k or A_k. In particular we have for L from (3.41)

$$L_0 = \eta^{-1}, \quad L_1 = 2(\cos\phi - \eta^{-1}), \quad L_2 = \eta^{-1}(1 + 2\delta_1) - 2\cos\phi + \eta. \tag{3.45}$$

Note that while the leading two terms for L are known in terms of the input parameters $\{\eta, \phi\}$, the later ones involve unknown coefficients δ_j for $\delta(Y_1)$. Then (3.43) implies that

$$C_{00} = \eta^{-1} A_{00} = \eta^{-1/2} K_0, \qquad C_{01} = -\eta^{-1} A_{01} = \eta^{1/2}(\cos\phi - \eta^{-1}) K_0. \tag{3.46}$$

We now turn to the vorticity equation (3.34) for C_0'. On the right-hand side, with our uniformity assumption we have $\hat{F}_r$, A_0 and C_0 expanding in inverse powers of Y_1 as $Y_1 \to \infty$, and so

$$\sum_{r=1}^{\infty} r^{-1} Y_1 [(\hat{F}_r - A_0) C_0]' = O(Y_1^{-1}), \quad Y_1 A_0' C_0 = O(Y_1^{-1}). \tag{3.47}$$

In this way, the head of the series $\hat{F}_r$, which is not accessible to us, fortunately drops out of the equation. We are left with just the terms $Y_1^2 C_0' \sim -C_{01}$ on the left-hand side, and $-A_0 C_0 \sim -A_{00} C_{00}$ on the right-hand as constants at leading order in the limit $Y_1 \to \infty$. We thus obtain the link

$$C_{01} = A_{00} C_{00} = K_0^2, \tag{3.48}$$

This implies that

$$K_0 = \eta^{1/2}(\cos\phi - \eta^{-1}). \tag{3.49}$$

and so all the leading terms in (3.46) are now fixed in terms of $\{\eta, \phi\}$. Going to the next order in powers of $Y_1 \gg 1$, (3.34) just links C_{02} to the head of the series for $\hat{F}_r$, and so does not yield useful information. Equations (3.43) give A_{02} and C_{02} in terms of δ_1 but with three unknowns and two equations, the system is not closed.

We can also look at C_1: equation (3.35) amounts to

$$Y_1 C_1' + C_1 = 0, \tag{3.50}$$

and is integrated as

$$C_1 = K_1 Y_1^{-1}, \tag{3.51}$$

where K_1 is a constant of integration. This gives $C_{11} = K_1$ and $C_{1j} = 0$ for $j \neq 1$. We can use (3.36–3.39) to fix other quantities from this, and we obtain

at leading orders

$$A_{10} = 0, \quad A_{11} = \eta K_1 + \eta^{1/2} K_0; \tag{3.52}$$

We have introduced a constant K_1 but it does not seem possible to fix it; the problem is that if one writes down the equation analogous to (3.34) for C_1 and looks at the large-Y_1 limit, the heads of the series are involved and so no general deductions can be made.

To summarise, in this section we have, based on a uniformity assumption, given the leading order structure of the vorticity and stream function prefactors A_0 and C_0 on the singular manifold, as $Y_1 \to \infty$, in terms of the input parameters $\{\eta, \phi\}$; see (3.46) in conjunction with (3.49). We have not yet restricted the value of ϕ to show that ϕ must be zero, and this is the aim of the next section.

4 Tying up the tails of the manifolds

We have so far focused on the right-hand tail of the singular manifold, that is, as $Y_1 \to \infty$ and Y_2 tending rapidly to zero according to

$$W_2 = Y_2 Y_1^{-1} e^{Y_1} = \Delta(Y_1) = \exp(\delta(Y_1)) \sim \exp(\delta_0 + \delta_1 Y_1^{-1} + \cdots). \tag{4.1}$$

However the singular manifold also has a left-hand tail and we can apply the same analysis here. In other words we may give the same development for quantities related by the mode relabelling, or tail-swapping, symmetry (2.22). The results from the two tails must match up and this further constrains the analysis. Specifically the asymptotic descriptions from either tail should match up in an overlap region, for example the region $-1 < W_1 < 1$ in figure 6.

Formally, we have used a bar over quantities to denote the operation of the symmetry (2.22) and we can use a similar bar over any other quantity, for example $\bar{\delta}$ or $\bar{C}$. With this, every equation has a barred counterpart, and we may also use Y_1 and $\bar{Y}_1 \equiv Y_2$ as a symmetrical set of coordinates. Thus for example we obtain from (4.1, $\overline{4.1}$),

$$\bar{Y}_1 = Y_1 e^{-Y_1} \Delta(Y_1) = Y_1 e^{-Y_1 + \delta(Y_1)}, \quad Y_1 = \bar{Y}_1 e^{-\bar{Y}_1} \bar{\Delta}(\bar{Y}_1) = \bar{Y}_1 e^{-\bar{Y}_1 + \bar{\delta}(\bar{Y}_1)}, \tag{4.2}$$

from which we have the relation

$$\delta(Y_1) + \bar{\delta}(\bar{Y}_1) = Y_1 + \bar{Y}_1. \tag{4.3}$$

Taking the derivative of the first of (4.2) involves a familiar quantity,

$$-\frac{Y_1}{\bar{Y}_1} \frac{d\bar{Y}_1}{dY_1} = -Y_1 \delta' + Y_1 - 1, \tag{4.4}$$

and from (3.41) it may be checked that

$$L = \left(\frac{d\bar{Y}_1}{dY_1}\right)^2 \bar{L}. \tag{4.5}$$

To make the tails agree we need to link the prefactors A_0 and C_0 to $\bar{A}_0$ and $\bar{C}_0$. The upshot of this will be that we can equate K_0 and $-\bar{K}_0$, which will close the problem and force $\phi = 0$. To do this, we first reconstruct the functions Ψ and Ω. We use the series (2.58–2.61), together with (3.8, 3.10) and the expansions (3.16, 3.18). In view of the following sums,

$$\sum_{n=0}^{\infty} z^n = (1-z)^{-1}, \quad \sum_{n=1}^{\infty} n^{-2} z^n = (1-z)\log(1-z) + \cdots \tag{4.6}$$

as $z \to 1$, we obtain the leading singular behaviour of Ψ and Ω near the manifold $W_2 = \Delta(Y_1)$ as

$$\Psi = Y_1^{-1} A_0(Y_1)(1 - W_2/\Delta(Y_1))\log(1 - W_2/\Delta(Y_1)) + \cdots, \tag{4.7}$$
$$\Omega = Y_1 C_0(Y_1)(1 - W_2/\Delta(Y_1))^{-1} + \cdots. \tag{4.8}$$

We want to equate the strengths of the singularities from each tail, so we work in the $(Y_1, \bar{Y}_1)$-plane. We fix $(Y_1, \bar{Y}_1)$ as a point on the singular manifold, and let s be an inward-pointing coordinate measuring distance perpendicular to the manifold at this point. A short calculation gives the local behaviour as a function of s by

$$\Psi = Y_1^{-1} A_0 [Y_1^{-2}(-Y_1\delta' + Y_1 - 1)^2 + \bar{Y}_1^{-2}]^{1/2}\, s \log s + \cdots, \tag{4.9}$$
$$\Omega = Y_1 C_0 [Y_1^{-2}(-Y_1\delta' + Y_1 - 1)^2 + \bar{Y}_1^{-2}]^{-1/2} s^{-1} + \cdots. \tag{4.10}$$

Note this confirms the vorticity dependence $\Omega = O(s^{-1})$ as the singular manifold is approached, corresponding to the exponent $\beta = 1$ in (3.6).

Now the same calculation applies with regard to the left-hand tail, by interchanging barred and unbarred quantities, with the same quantity s. In view of the symmetry (2.22), specifically $\bar{\Psi} = -\Psi$ and $\bar{\Omega} = -\Omega$ we can equate the strengths of the singularities from the two tails to yield, schematically

$$Y_1^{-1} A_0 [\leftrightarrow]^{1/2} = -\bar{Y}_1^{-1} \bar{A}_0 [\overleftrightarrow]^{1/2}, \tag{4.11}$$
$$Y_1 C_0 [\leftrightarrow]^{-1/2} = -\bar{Y}_1 \bar{C}_0 [\overleftrightarrow]^{-1/2}. \tag{4.12}$$

where $[\leftrightarrow]$ denotes the common bracketed quantity in (4.9, 4.10). Multiplying these two together gives

$$A_0 C_0 = \bar{A}_0 \bar{C}_0. \tag{4.13}$$

and so from (3.42), $K_0^2 = \bar{K}_0^2$. In fact we require $K_0 = -\bar{K}_0$ and in view of (2.22, 3.49) we then have

$$K_0 = \eta^{1/2}(\cos\phi - \eta^{-1}) = -\bar{K}_0 = -\eta^{-1/2}(\cos\phi - \eta). \tag{4.14}$$

For this to be satisfied, $\cos\phi = 1$ and so $\phi = 0$. We have thus shown that our expansions with an exponent $\alpha = 0$, and the key uniformity assumption, are only compatible with $\phi = 0$. With this holding, we have fixed the leading behaviour of C_0 and A_0 in the tails. We will confirm this in the next section.

Note that if we instead take the ratio of (4.11) and (4.12) we have

$$Y_1^2 L\,[\leftrightarrow]^{-1} = \bar{Y}_1^2 \bar{L}\,[\rightleftarrows]^{-1}. \tag{4.15}$$

However this contains nothing new (only a check on the calculations) in view of (4.5) and the fact that

$$[\leftrightarrow] = \bar{Y}_1^{-2}\left(\frac{d\bar{Y}_1}{dY_1}\right)^2 + \bar{Y}_1^{-2} = [\rightleftarrows]\left(\frac{Y_1}{\bar{Y}_1}\frac{d\bar{Y}_1}{dY_1}\right)^2. \tag{4.16}$$

We conclude that all the useful information from matching the tails is contained in (4.13).

Finally in this section we note that the limit $Y_1 \to \infty$ is equivalent to $\bar{Y}_1 \equiv Y_2 \to 0$, and so from the behaviour of Δ, A_0 and C_0 as $Y_1 \to \infty$ we can obtain information about $\bar{\Delta}_0$, $\bar{A}_0$ and $\bar{C}_0$ as $\bar{Y}_1 \to 0$. The link between Y_1 and $\bar{Y}_1$ in the first of (4.2) may be inverted as

$$Y_1 = \log\bar{Y}_1^{-1} + \log(\log\bar{Y}_1^{-1}) + \delta_0 + \cdots; \tag{4.17}$$

Y_1 is only logarithmic in $\bar{Y}_1$. We can write from (4.4, 4.5)

$$\bar{A}_0 = \bar{K}_0\bar{L}^{-1/2} = \bar{K}_0 Y_1^{-1}\bar{Y}_1(-Y_1\delta' + Y_1 - 1)L(Y_1)^{-1/2} \sim \eta^{1/2}\bar{K}_0\bar{Y}_1 \tag{4.18}$$

$$\bar{C}_0 = \bar{K}_0\bar{L}^{1/2} = \bar{K}_0 Y_1\bar{Y}_1^{-1}(-Y_1\delta' + Y_1 - 1)^{-1}L(Y_1)^{1/2} \sim \eta^{-1/2}\bar{K}_0\bar{Y}_1^{-1} \tag{4.19}$$

using (3.45). Exchanging barred and unbarred quantities gives the leading small-Y_1 behaviour of A_0 and C_0 as

$$A_0 \sim \eta^{-1/2}K_0 Y_1, \quad C_0 \sim \eta^{1/2}K_0 Y_1^{-1} \qquad (Y_1 \to 0). \tag{4.20}$$

Corrections to this involve $\bar{Y}_1$, which is of order $\log Y_1$ and so convergence to these asymptotic forms is likely to be rather slow. We also note that whereas our key assumption was uniform convergence to the asymptotic forms for large Y_1, this is unlikely to occur for small Y_1 and in fact does not as we shall see.

5 Exact solutions

Our aim in this section is to confirm the asymptotic framework above for the case $\phi = 0$. The key result is that the exponent $\alpha = 0$, together with $\beta = 1$ and $\alpha_{\rm PMFB} = 5/2$, gives a consistent asymptotic picture of the singular manifold. The following quantities are pinned down from $K_0 = \eta^{1/2} - \eta^{-1/2}$ in (3.49),

$$\eta C_{00} = A_{00} = \eta - 1, \quad \eta C_{01} = -A_{01} = (\eta - 1)^2, \tag{5.1}$$

as terms in the large-Y_1 expansions (3.44) of the leading vorticity and stream function prefactors A_0 and C_0; see (3.46). We also have, as $Y_1 \to \infty$ for the next correction,

$$C_1 = K_1 Y_1^{-1}, \quad A_1 \sim (\eta K_1 + \eta - 1) Y_1^{-1} \qquad (Y_1 \to \infty), \tag{5.2}$$

from (3.51), with K_1 unknown to us. Finally we have for the small-Y_1 behaviour,

$$A_0 \sim (1 - \eta^{-1}) Y_1, \quad C_0 \sim (\eta - 1) Y_1^{-1} \qquad (Y_1 \to 0), \tag{5.3}$$

from (4.20). We originally tested these predictions from the numerical solution of the $\{f_n, h_n\}$ or $\{F_n, H_n\}$ hierarchies. However it became apparent that exact solutions are available in the case $\phi = 0$ and we will use these. The results in this section were obtained with the assistance of Maple and Mathematica.

Note that we have already studied the small-Y_1 behaviour of each third order system (f_n, h_n) (2.36–2.38) in the absence of forcing, $s_n = 0$, and given the three forms of the solution in (2.41, 2.42). Although each system may be integrated in terms of hypergeometric functions, because of generally oscillatory behaviour near the origin in (2.42), it is pretty clear that the solutions are not likely to simplify to anything useful unless $\phi = 0$ or $\phi = \pi$.

So we fix $\phi = 0$ and consider the homogeneous system for (f_n, h_n) with $s_n = 0$ and any value of η. We set $Y \equiv Y_1$ for brevity in what follows. Two solutions can be written as

$$f_n = (Y + \eta - 1) Y^{-n\eta}, \quad h_n = \eta^{-1} Y^{-n\eta + 1} \tag{5.4}$$

and (omitting h_n for brevity)

$$f_n = (Y + \eta - 1) Y^{-n\eta} \int_0^{nY} r^{n(\eta-1)} e^r \, dr - n^{n(\eta-1)} Y^{-n+1} e^{nY} \tag{5.5}$$

(involving an incomplete gamma function). A third solution can be written down in tems of hypergeometric functions, but this is singular at the origin, and so we do not give it here. The solution for (f_1, h_1) that satisfies the boundary condition (2.40) is $-\eta$ times (5.5). The forced problem does not appear to have explicit solutions for general values of η.

However there are significant simplifications when η is an integer (with still $\phi = 0$). In this case the solutions above become sums of products of exponentials times powers of Y. With some experimentation it is apparent that the $\{f_n, h_n\}$ hierarchy, including the forcing term s_n, can be solved order by order in terms of a finite [1] collection of such functions, of the general form:

$$f_n = \sum_{j=0}^{n\eta} \sum_{k=0}^{n} f_{njk}\, Y^{-j} e^{kY}, \quad h_n = \sum_{j=0}^{n\eta} \sum_{k=0}^{n} h_{njk}\, Y^{-j} e^{kY} \tag{5.6}$$

(many coefficients being zero). For $\eta = 2$ we obtain for the first few,

$$f_1 = 2Y^{-2}e^Y - 2Y^{-1} - 2Y^{-2}, \tag{5.7}$$

$$h_1 = \left(1 + Y^{-1}\right) e^Y - Y^{-1}, \tag{5.8}$$

$$f_2 = \left(Y^{-3} - 3Y^{-4}\right) e^{2Y} + 4Y^{-3}e^Y + Y^{-3} + 3Y^{-4}, \tag{5.9}$$

$$h_2 = \left(2Y^{-1} - 3Y^{-2} - \frac{5}{2}Y^{-3}\right) e^{2Y} + \left(2Y^{-1} + 6Y^{-2} + 2Y^{-3}\right) e^Y + \frac{1}{2}Y^{-3}, \tag{5.10}$$

$$f_3 = \left(\frac{8}{9}Y^{-4} - \frac{122}{27}Y^{-5} + \frac{160}{27}Y^{-6}\right) e^{3Y} + \left(4Y^{-4} - 10Y^{-5}\right) e^{2Y} + \left(4Y^{-4} - 2Y^{-5}\right) e^Y - \frac{34}{27}Y^{-5} - \frac{160}{27}Y^{-6}, \tag{5.11}$$

$$h_3 = \left(4Y^{-2} - \frac{41}{3}Y^{-3} + \frac{73}{9}Y^{-4} + \frac{179}{27}Y^{-5}\right) e^{3Y} + \left(8Y^{-2} - 22Y^{-4} - 5Y^{-5}\right) e^{2Y} + \left(2Y^{-2} + 9Y^{-3} + 5Y^{-4} - Y^{-5}\right) e^Y - \frac{17}{27}Y^{-5}, \tag{5.12}$$

$$f_4 = \left(Y^{-5} - \frac{125}{18}Y^{-6} + \frac{3533}{216}Y^{-7} - \frac{105}{8}Y^{-8}\right) e^{4Y} + \left(\frac{16}{3}Y^{-5} - \frac{212}{9}Y^{-6} + \frac{716}{27}Y^{-7}\right) e^{3Y} + \left(8Y^{-5} - 18Y^{-6} + 5Y^{-7}\right) e^{2Y} + \left(\frac{8}{3}Y^{-5} - 4Y^{-6} + \frac{68}{27}Y^{-7}\right) e^Y + \frac{455}{216}Y^{-7} + \frac{105}{8}Y^{-8}, \tag{5.13}$$

$$h_4 = \left(8Y^{-3} - \frac{374}{9}Y^{-4} + \frac{3559}{54}Y^{-5} - \frac{83}{4}Y^{-6} - \frac{7807}{432}Y^{-7}\right) e^{4Y} + \left(24Y^{-3} - 50Y^{-4} - \frac{100}{3}Y^{-5} + \frac{650}{9}Y^{-6} + \frac{358}{27}Y^{-7}\right) e^{3Y} + \left(16Y^{-3} + 20Y^{-4} - 44Y^{-5} - 21Y^{-6} + \frac{5}{2}Y^{-7}\right) e^{2Y} + \left(\frac{4}{3}Y^{-3} + \frac{22}{3}Y^{-4} + \frac{88}{27}Y^{-5} - \frac{38}{9}Y^{-6} + \frac{34}{27}Y^{-7}\right) e^Y + \frac{455}{432}Y^{-7}. \tag{5.14}$$

[1] Note that for non-integer values of η polynomials in Y^{-1} in the expressions below would be replaced by asymptotic series in Y^{-1}.

We observe that the leading terms as $Y \to \infty$ are (as seen above),

$$f_n \sim n^{-2}\, 2^n Y^{-n-1} e^{nY}, \quad h_n \sim 2^{n-1} Y^{-n+1} e^{nY}. \tag{5.15}$$

In fact further exploration with computer algebra and other, integer values of η up to $\eta = 6$ are consistent with the following

$$f_n = n^{-2}(\eta-1)\eta^n Y^{-n-1} e^{nY}, \quad h_n = (\eta-1)\eta^{n-1} Y^{-n+1} e^{nY}. \tag{5.16}$$

In view of (2.46, 3.8–3.10, 3.16–3.18), this indicates that we have $\alpha = 0$ and

$$\delta_0 = \log \eta^{-1}, \quad A_{00} = \eta - 1, \quad C_{00} = 1 - \eta^{-1}, \quad A_{j0} = 0, \quad C_{j0} = 0 \quad (j \geq 1). \tag{5.17}$$

These results for A_{00} and C_{00} confirm (5.1) while the zero values of A_{10} and C_{10} are consistent with (5.2). Note that we have not pursued our expansions to find out information about A_j or C_j for $j \geq 1$ and also that the above, intriguingly simple, values of δ_0 are not accessible to us within the asymptotic framework [2] .

To go further we need to extract C_0 and C_1 for a range of Y-values, not just the limiting case $Y \to \infty$. To do this obtain H_n from h_n and write

$$H_n = e^{-n\delta}[C_0 + n^{-1} C_1 + O(n^{-2})] \tag{5.18}$$

in the form

$$\log H_n = -n\delta + \log C_0 + n^{-1} C_1/C_0 + O(n^{-2}). \tag{5.19}$$

Use of three adjacent values of n enables us to extract approximations to δ, $\log C_0$ and C_1/C_0

$$\begin{pmatrix} \delta^{(n)} \\ \log C_0^{(n)} \\ C_1^{(n)}/C_0^{(n)} \end{pmatrix} \simeq \tfrac{1}{2} \begin{pmatrix} -(n-1) & 2n & -(n+1) \\ -(n-1)(2n+1) & 4n^2 & -(n+1)(2n-1) \\ n(n^2-1) & -2n(n^2-1) & n(n^2-1) \end{pmatrix} \begin{pmatrix} \log H_{n-1} \\ \log H_n \\ \log H_{n+1} \end{pmatrix}. \tag{5.20}$$

We can similarly obtain $A_0^{(n)}$ and $A_1^{(n)}$ from adjacent $n^2 F_n$. Use of computer algebra to expand the results for large Y_1 gives approximations to A_{01}, C_{01}, A_{11} and C_{11}. Our results for varying η and n may be summarised as

$$A_{01}^{(n)} = -(\eta-1)^2\, \frac{2n^2+1}{2n^2}, \quad C_{01}^{(n)} = \frac{(\eta-1)^2}{\eta}\, \frac{2n^2-1}{2n^2}, \tag{5.21}$$

confirming (5.1) as $n \to \infty$, and

$$A_{11}^{(n)} = \frac{[(\eta+1)^2-4]n + (\eta-1)^2}{2n}, \quad C_{11}^{(n)} = \frac{(\eta^2-1)n + (\eta-1)^2}{2\eta n}, \tag{5.22}$$

[2] These values of δ_0 are also found in the passive scalar model discussed in PMFB.

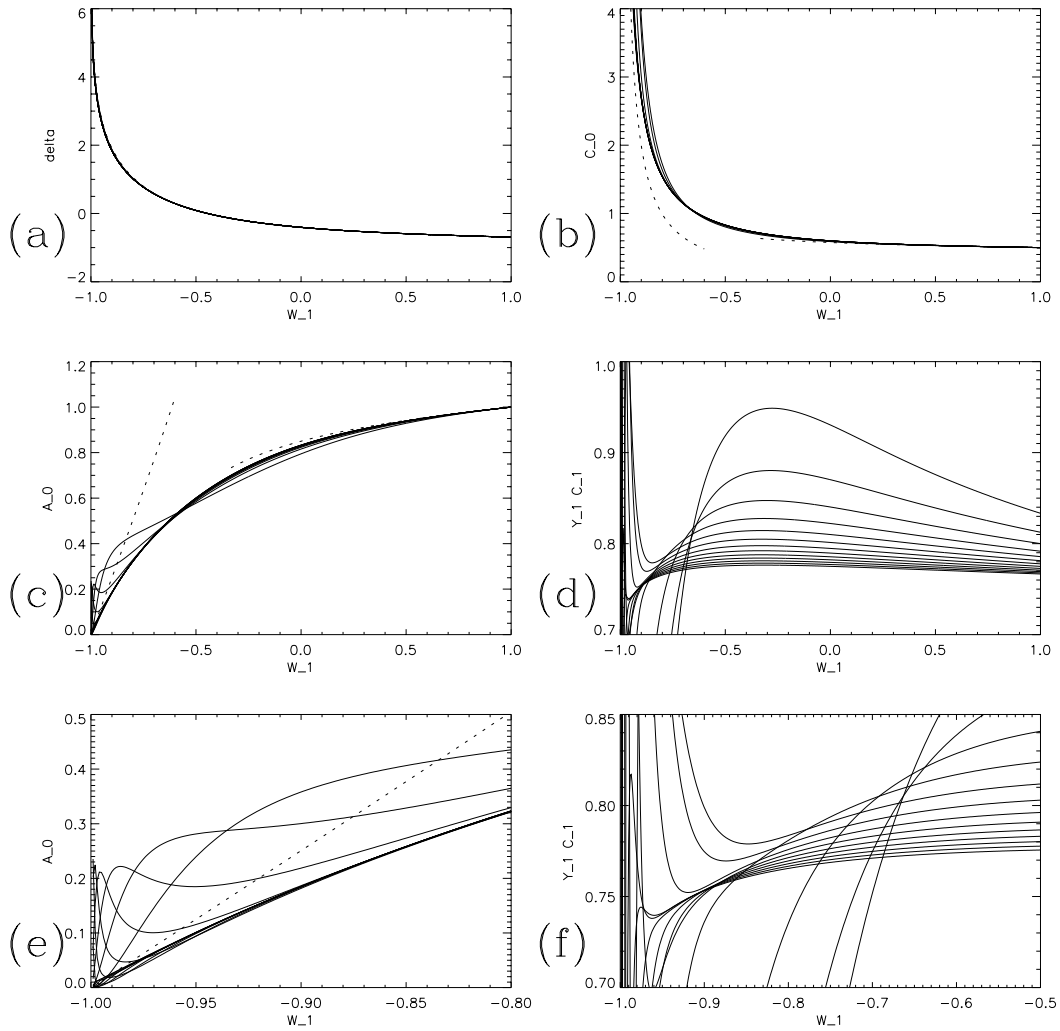

Fig. 7. Plotted are the approximations (a) $\delta^{(n)}$, (b) $C_0^{(n)}$, (c) $A_0^{(n)}$, and (d) $YC_1^{(n)}$ against W_1, obtained for $\eta = 2$ and $n = 2, 3, \ldots 15$. In (b,c) asymptotic forms are shown dotted. Panels (e,f) are blow-ups of (c,d) near the origin.

in agreement with (5.2) for

$$K_1 = \tfrac{1}{2}(\eta - \eta^{-1}), \tag{5.23}$$

a quantity for which we have no analytical prediction.

Finally we can use this scheme to plot approximations $\delta^{(n)}$, $C_0^{(n)}$, $A_0^{(n)}$ and $C_1^{(n)}$ against W_1 for increasing values of n. The functions are calculated using high precision arithmetic in Maple and are shown for $\eta = 2$ and 3 in figures 7 and 8. In (a) calculations of $\delta^{(n)}$ from H_n are shown solid, and from F_n are shown dotted, but are barely distinguishable. Panels (b,c) of each figure have the large-Y forms from (5.1) and small-Y forms (5.3) shown dotted: the uniform convergence for large Y and non-uniform convergence for small Y are apparent. Panels (d) show YC_1 plotted against W_1: this should tend to a

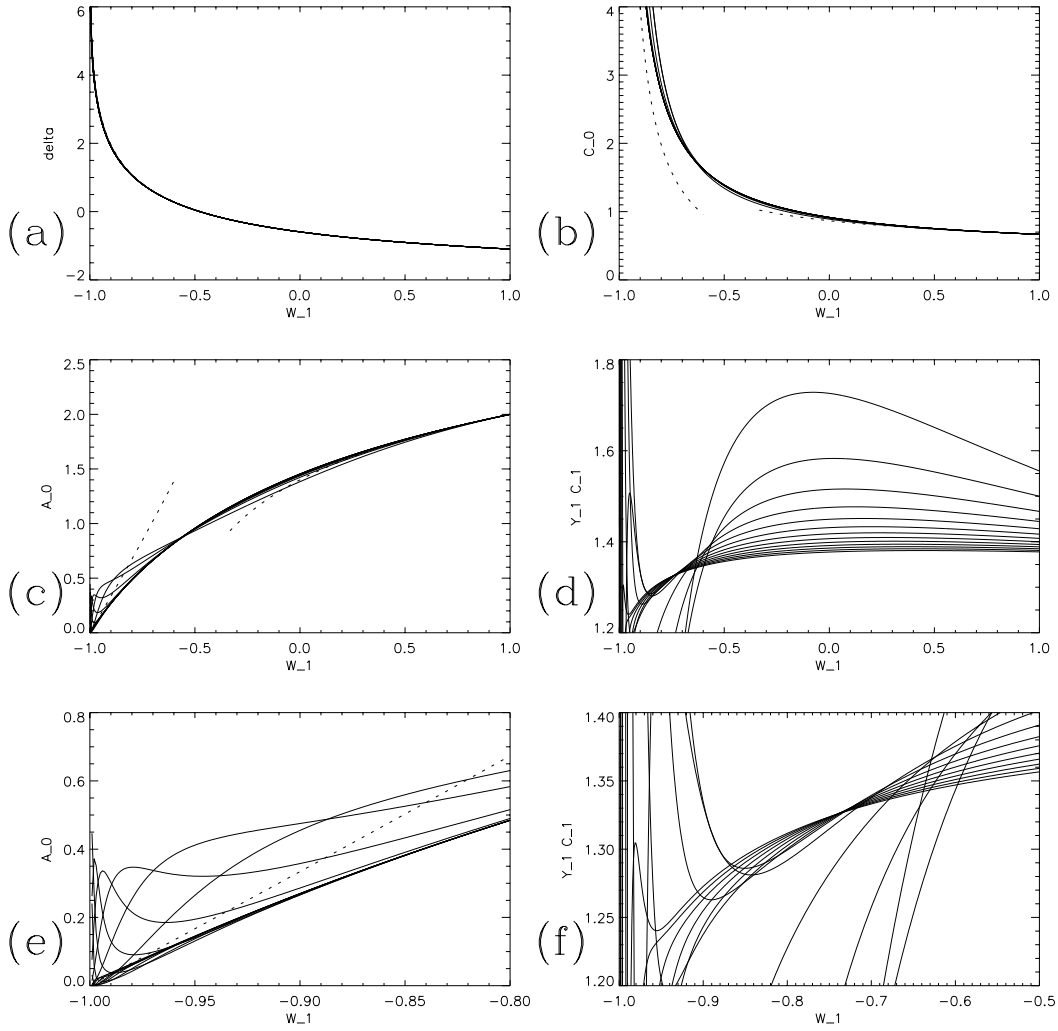

Fig. 8. As in figure 7 but for $\eta = 3$.

constant K_1 across the whole range of Y and appears to be doing so in each case, though again slowly and non-uniformly for small Y. Finally panels (e,f) are blow-ups of (c,d) near the origin.

6 Discussion and outlook

We have studied the problem of complex singularities in the Euler equation with an initial condition of two complex modes parameterised by $\{\eta, \phi\}$ where η is the ratio of the wave numbers and ϕ the angle between the modes. The vorticity is known to diverge on a singular manifold, obtained by analytically extending the usual spatial variables. Our goal is to obtain the vorticity scaling exponent $\beta(\eta, \phi)$ as a function of these parameters, or equivalently $\alpha(\eta, \phi) = 1 - \beta$. This remains out of our reach. What we have done in this paper is to present an asymptotic framework consistent with the result $\beta(\eta, 0) = 1$. This

is not a rigorous proof, but is formal asymptotics backed up with numerical simulations and computer algebra. Nonetheless it is in agreement with the results of WP who finds $\beta = 1$ in this case to a very high degree of accuracy [3]. The exponent is independent of η, in agreement with PMFB, who find that scaling exponents appear to depend only on ϕ in their numerical studies.

Our result that $\beta = 1$ corresponds only to $\phi = 0$ within our framework is also consistent with PMFB and WP who find values of β that are less than unity for angles that include $\phi = \pi/4$, $\pi/2$ and π. However we cannot say that our framework gives a proof that $\phi \neq 0$ implies $\beta < 1$, as it is possible that we simply have not been ingenious enough in our expansions, or that the uniformity assumption could need to be relaxed in some way. In short, while we have a consistent formal framework for the $\phi = 0$, $\beta = 1$ case, it is just that, and we are not able to say much about what lies outside it without extending it in some way, relaxing some of our assumptions or expansions.

We are now investigating the case $\alpha \neq 0$ and so aiming to extend our analysis to $\phi \neq 0$ using the expansions (3.1). There remain a number of unresolved issues, though. Some components of the discussion go through as before, for example the link between A_0 and C_0 through the Laplacian, equations (3.36–3.41), and the result (4.13) becomes

$$A_0^{1-\alpha} C_0^{1+\alpha} Y_1^{2\alpha} = \bar{A}_0^{1-\alpha} \bar{C}_0^{1+\alpha} \bar{Y}_1^{2\alpha}. \tag{6.1}$$

However problems arise in the effect of summing the quadratic, nonlinear interactions. We have general sums now of the form

$$\Sigma_{P,Q} = \sum_{r=1}^{n-1} r^{-\alpha-P} (n-r)^{-\alpha-Q} \qquad (P, Q \geq 0), \tag{6.2}$$

to deal with for $\alpha > 0$. For $\alpha = 0$ we obtained a leading logarithmic term in $\Sigma_{1,0}$ (3.28). This term (which crucially comes from the tails of the series and not the heads) appeared at order $n^{-1} \log n$ in (3.33) where we had no choice but to set it to zero and obtain the key relation (3.42) on which the rest of the analysis hangs.

For $\alpha > 0$ the corresponding term from the tails of the series appears at order $n^{-1-\alpha}$ relative to (3.33–3.35), which is subdominant to the leading, order n^{-1} term that depends on the head of the series and is linked to C_0'. Because it is subdominant, there is no obvious reason why it should be zero, and the mathematical development falters at this point. With this, since the asymptotic expansion appears to be separated by powers of $n^{-\alpha}$ with modest values of α, we expect extremely slow approach to the asymptotic limit as $n \to \infty$, and

[3] The limiting case $\phi = 0$ can also be considered for the Navier–Stokes equations with properly rescaled time and viscosity, but this problem will be studied elsewhere.

probably failure of our uniformity assumption. This is of course seen in PMFB and WP, where numerical approaches are used to enhance convergence and provide the estimates (3.4, 3.5) for α. Suffice it to say that with the limited values of n that we can achieve in solving the hierarchy of ODEs, there is little numerical guidance within our framework as to the correct asymptotic picture, and relating α to ϕ remains an open problem.

Looking further ahead, the above work is just for two modes and a real initial condition such as (2.24) will involve four modes and angles ϕ and $\pi - \phi$, with several pieces of complex manifold that interact as t increases. The question is whether the interaction tends to enhance or deplete the nonlinearity,together with the motion of the singularities to the real axis and so the formation of small scales. Further studies should also develop theory in three dimensions, to study the interaction of three modes with the use of the tools developed here and numerics analogous to PMFB; see Pauls (2007). Finally, in this article we have looked at complex singularities of flows on a two-dimensional torus. Recently, in Li & Sinai (2008) complex singularities of viscous three-dimensional [4] flows in $\mathbb{R}^3$ have been studied by a renormalisation group method. In contrast to the two-mode initial conditions used here, Li and Sinai consider initial conditions compactly supported around one mode, which corresponds to the case $\phi = 0$, and prove existence of complex singularities as well as determine their scaling. In principle, for the same kind of initial conditions one could also consider complex singularities of the Euler equation. However, because of the absence of viscosity the renormalisation group approach does not work in the inviscid case, and so other methods are required. Nevertheless, we expect that the scaling found in this setting will correspond to $\beta = 1$ found in the present study.

Acknowledgements

ADG is grateful for the award of a Levehulme Trust Research Fellowship, which supported this research. WP woud like to acknowledge support from the research project OTARIE (ANR-07-BLAN-0235 OTARIE). Both authors thank Uriel Frisch for introducing them to this intriguing problem and for numerous valuable discussions and references. We also thank Andrew Bassom and Matthew Turner for helpful comments during this research.

[4] Note that their renormalisation group method can also be extended to viscous flows in dimension $d \geq 2$.

A Evaluation of sums

Here we give detailed justification of the formulae (3.30–3.32) which are derived using (3.26–3.29). We first look at $\hat{S}_n^{\mathrm{I}}$ in (3.22). Contributions from the tails of the series for $\hat{F}_n$ and $\hat{H}_n$ are given by substituting $A_P n^{-P}$ and $C_Q n^{-Q}$ respectively to give a general tail term of the form

$$n^{-1}\Sigma_{1+P,Q}\, Y_1 (A_P C_Q)'. \tag{A.1}$$

The case $P = Q = 0$ gives a term of order $n^{-1}\log n$ and $P = 0$, $Q = 1$ gives a term of order $n^{-2}\log n$. Terms with $Q = 0$ and $P \geq 1$ are of size n^{-1}, while all the remaining terms are of order n^{-2} or smaller. This indicates that we may approximate $\hat{S}_n^{\mathrm{I}}$ as

$$\begin{aligned}\hat{S}_n^{\mathrm{I}} &= n^{-1}\Sigma_{1,0}\, Y_1 (A_0 C_0)' + n^{-1}\Sigma_{1,1}\, Y_1 (A_0 C_1)' \\ &\quad + n^{-1}\sum_{r=1}^{n-1} r^{-1} Y_1 [(\hat{F}_r - A_0)C_0]' + O(n^{-2}).\end{aligned} \tag{A.2}$$

Use of (3.28, 3.29) then gives (3.30). To be completely clear, the terms that have been omitted are

$$n^{-1}\sum_{r=1}^{n-1} r^{-1}(n-r)^{-1} Y_1 [(\hat{F}_r - A_0)C_1]' = O(n^{-1}\Sigma_{2,1}) = O(n^{-2}), \tag{A.3}$$

$$n^{-1}\sum_{r=1}^{n-1} r^{-1} Y_1 [\hat{F}_r (\hat{H}_{n-r} - C_0 - C_1 (n-r)^{-1})]' = O(n^{-1}\Sigma_{1,2}) = O(n^{-2}), \tag{A.4}$$

and in going to (3.30) we have also neglected a term

$$n^{-1}\sum_{r=n}^{\infty} r^{-1} Y_1 [(\hat{F}_r - A_0)C_0]' = O(n^{-2}). \tag{A.5}$$

We now consider $\hat{S}_n^{\mathrm{II}}$ in (3.22). If we focus on the tails of the distributions and substitute A_0 for $\hat{F}_n$ and $C_0 + C_1 n^{-1}$ for $\hat{H}_n$, we obtain a term of the form

$$\hat{S}_n^{\mathrm{II}} = n^{-1}\Sigma_{1,1}\,(Y_1 A_0' - A_0)C_1 = O(n^{-2}\log n). \tag{A.6}$$

In fact this term is the largest and by virtue of (3.29) we obtain the approximation (3.31). Specifically we have omitted the following terms in making this

approximation,

$$n^{-1}\sum_{r=1}^{n-1} r^{-1}(n-r)^{-1}(Y_1\hat{F}_r' - \hat{F}_r - Y_1A_0' + A_0)C_1$$
$$= O(n^{-1}\Sigma_{2,1}) = O(n^{-2}), \tag{A.7}$$
$$\sum_{r=1}^{n-1} r^{-1}(n-r)^{-1}(Y_1\hat{F}_r' - \hat{F}_r)[\hat{H}_{n-r} - \hat{H}_n - C_1(n-r)^{-1} + C_1n^{-1}]$$
$$= O(n^{-1}\Sigma_{1,2}, n^{-2}\Sigma_{0,2}) = O(n^{-2}). \tag{A.8}$$

$\hat{S}_n^{\mathrm{III}}$ in (3.22) is easy to deal with as it involves only the tails of the expansions for $\hat{F}_n$ and $\hat{H}_n$, and we obtain

$$\hat{S}_n^{\mathrm{III}} = \Sigma_2(Y_1A_0' - A_0)C_0 + O(n^{-2}), \qquad \Sigma_P \equiv \sum_{r=n}^{\infty} r^{-P}, \tag{A.9}$$

which then gives (3.32).

Recall also that in equations (3.33, 3.35) we set the left hand side to zero, and this gave us key relations in our asymptotic description. We could alternatively have attempted to introduce non-zero terms on the left-hand side and included them in the series for the vorticity. Here we consider what would happen were we to follow this route. Specifically consider (3.33): if we had allowed this to drive a term $C_{0\mathrm{L}}\log n$ in the series (3.18), we would also need a term $A_{0\mathrm{L}}\log n$ in (3.16). We would then have a term in $\hat{S}_n^{\mathrm{I}}$ of the form $n^{-1}\Sigma_{1\mathrm{L},0\mathrm{L}}Y_1(A_{0\mathrm{L}}C_{0\mathrm{L}})'$ (cf. (A.1)) with

$$\Sigma_{1\mathrm{L},0\mathrm{L}} = \sum_{r=1}^{n-1} r^{-1}\log r\log(n-r). \tag{A.10}$$

By the Euler summation formula, the behaviour of this is linked to the integral

$$\int s^{-1}\log s\log(1-s)\,ds = \mathrm{polylog}(3,s) - \log s\,\mathrm{polylog}(2,s). \tag{A.11}$$

This introduces polylogarithm functions

$$\mathrm{polylog}(a,s) = \sum_{n=1}^{\infty} s^n n^{-a}, \tag{A.12}$$

and we would have to include further terms in the series expansion (3.16–3.18) as $n \to \infty$.

Similarly if we allow the equation (3.35) to drive a term $C_{1\mathrm{L}}n^{-1}\log n$ in the series (3.18), we would then have a term in $\hat{S}_n^{\mathrm{I}}$ of the form $n^{-1}\Sigma_{1,1\mathrm{L}}Y_1(A_0C_{1\mathrm{L}})'$ with

$$\Sigma_{1,1\mathrm{L}} = \sum_{r=1}^{n-1} r^{-1}(n-r)^{-1}\log(n-r). \tag{A.13}$$

The behaviour of this is linked to

$$\int s^{-1}(1-s)^{-1}\log(1-s)\,ds = -\operatorname{polylog}(2,s) - \tfrac{1}{2}(\log(1-s))^2, \qquad \text{(A.14)}$$

which again introduces more functional dependence. Although we cannot rule out analytically that a more sophisticated expansion than (3.18) could hold, it is clear that this could only be achieved with significantly more complexity than that adopted by us, which in any case is confirmed in section 5.

References

Bardos, S. & Benachour, S. 1977 Domaine d'analyticité des solutions de l'équation d'Euler dans un ouvert de R^3. *Ann. Scuola Norm. Sup. Pisa* **4**, 647–687.

Beale, J.T., Kato, T. & Majda, A. 1984 Remarks on the breakdown of smooth solutions for the 3-D Euler equations. *Comm. Math. Phys.* **94**, 61–66.

Benachour, S. 1976 Analyticité des solutions périodiques de l'équation d'Euler en trois dimensions. *C.R. Acad. Sci. Paris A* **283**, 107–110.

Benachour, S. 1979 Analyticité des solutions des équations d'Euler. *Arch. Rat. Mech. Anal.* **71**, 271–299.

Brachet, M.E., Meiron, D.I., Orszag, S.A., Nickel, B.G., Morf, R.H. & Frisch, U. 1983 Small-scale structure of the Taylor–Green vortex *J. Fluid Mech.* **130**, 411–452.

Brachet, M.E., Meneguzzi, M., Vincent, A., Politano, H. & Sulem, P.-L. 1992 Numerical evidence of smooth self-similar dynamics and possibility of subsequent collapse for three-dimensional ideal flows. *Phys. Fluids A* **4**, 2845–2854

Bustamante, M.D. & Kerr, R.M. 2008 3-D Euler about a 2-D symmetry plane. *Physica D* **237**, 1912–1920.

Caflisch, R.E. 1993 Singularity formation for complex solutions of the 3D incompressible Euler equations. *Physica D* **67**, 1–18.

Chae, D. 2006 On the finite-time singularities of the 3-D incompressible Euler equations. *Comm. Pure Appl. Math.* **60**, 597–617.

Childress, S. 2008 Growth of anti-parallel vorticity in Euler flows. *Physica D* **237**, 1921–1925.

Cichowlas, C. & Brachet, M.-E. 2005. Evolution of complex singularities in Kida–Pelz and Taylor–Green inviscid flows *Fluid Dynam. Res.* **36**, 239–248.

Constantin, P. 2007 On the Euler equations of incompressible fluids. *Bull. Am. Math. Soc.* **44**, 603–621.

Deng, J., Hou, T.Y. & Yu, X. 2005 Geometric properties and nonblowup of 3-D incompressible Euler flow. *Commun. PDEs* **30**, 225–243.

Frisch, U., Matsumoto, T. & Bec, J. 2003 Singularities of Euler flow? Not out of the blue! *J. Stat. Phys.* **113**, 761–781.

Gibbon, J.D. 2008 The three-dimensional Euler equations: where do we stand? *Physica D* **237**, 1894–1904.

Gibbon, J.D., Bustamante, M. & Kerr, R.M. 2008 The three-dimensional Euler equations: singular or non-singular? *Nonlinearity* **2008**, T123–129.

Grafke, T., Homann, H., Dreher, J. & Grauer, R. 2008 Numerical simulations of possible finite time singularities in the incompressible Euler equations: comparison of numerical methods. *Physica D* **237**, 1932–1936.

He, X. 2007 An example of finite-time singularities in the 3d Euler equations. *J. Math. Fluid Mech.* **9**, 398–410.

Hou, T.Y. & Li, R. 2006 Dynamic depletion of vortex stretching and non-blowup of the 3-D incompressible Euler equations. *J. Nonl. Sci.* **16**, 639–664.

Hou, T.Y. & Li, R. 2008 Blowup or no blowup? The interplay between theory and numerics. *Physica D* **237**, 1937–1944.

Kerr, R.M. 2005 Velocity and scaling of collapsing Euler vortices. *Phys. Fluids* **17**, 075103, 1–11.

Kida, S. 1985 Three dimensional periodic flows with high symmetry. *J. Phys. Soc. Japan* **54**, 2132–2136.

Li, D. & Sinai, Ya.G. 2008 Blow ups of complex solutions of the 3D Navier–Stokes system and renormalization group method. *J. Eur. Math. Soc.* **10**, 267–313.

Matsumoto, T., Bec, J. & Frisch, U. 2005 The analytic structure of 2D Euler flow at short times. *Fluid Dynam. Res.* **36**, 221–237.

Matsumoto, T., Bec, J. & Frisch, U. 2008 Complex-space singularities of 2D Euler flow in Lagrangian coordinates. *Physica D* **237**, 1951–1955.

Moffatt, H.K. 2000 The interaction of skewed vortex pairs: a model for blow-up of the Navier–Stokes equations. *J. Fluid Mech.* **409**, 51–68.

Pauls, W. 2007 Singularités complexes des écoulements incompressibles parfaits. PhD thesis, University of Nice–Sophia Antipolis.

Pauls, W. 2009 On complex singularities of the 2D Euler equation at short times. *Physica D*, submitted, referred to as WP in the text. arXiv:0903.3161

Pauls, W. & Matsumoto, T. 2005 Lagrangian singularities of steady two-dimensional flow. *Geophys. Astrophys. Fluid. Dynam.* **99**, 61–75.

Pauls, W., Matsumoto, T., Frisch, U. & Bec, J. 2006 Nature of complex singularities for the 2D Euler equations. *Physica D* **219**, 40–59, referred to as PMFB in the text.

Pelz, R.B. & Gulak, Y. 1997 Evidence for a real-time singularity in hydrodynamics from time series analysis. *Phys. Rev. Lett.* **79**, 4998–5001.

Pelz, R.B. 2001 Symmetry and the hydrodynamic blow-up problem. *J. Fluid Mech.* **444**, 299–320.

Sulem, C., Sulem, P.-L. & Frisch, H. 1983 Tracing complex singularities with spectral methods *J. Comp. Phys.* **50**, 138–161.

Taylor, G.I. & Green, A.E. 1937 Mechanism of the production of small eddies from larger ones. *Proc. R. Soc. Lond. A* **158**, 499–521.